

# THE EVOLUTION OF EARLY-TYPE GALAXIES IN DISTANT CLUSTERS III.: $M/L_V$ RATIOS IN THE $Z = 0.33$ CLUSTER CL1358+62<sup>1,2</sup>

DANIEL D. KELSON<sup>3,4</sup>, GARTH D. ILLINGWORTH<sup>4</sup>, PIETER G. VAN DOKKUM<sup>5,6</sup>, AND MARIJN FRANX<sup>6</sup>

*Draft version November 8, 2018*

## ABSTRACT

Internal kinematics, length scales, and surface brightnesses, have been determined for a large sample of 53 galaxies in the cluster CL1358+62 at  $z = 0.33$  from Keck spectroscopy and *Hubble Space Telescope* WFPC2 imaging over a  $1.5h^{-1} \times 1.5h^{-1}$  Mpc<sup>2</sup> field of view. These data have been used to constrain the evolution of early-type galaxies in the cluster environment.

We have constructed the fundamental plane using E and S0 galaxies and draw the following conclusions. The fundamental plane at  $z = 0.33$  has the following form:  $r_e \propto \sigma^{1.31 \pm 0.13} \langle I \rangle_e^{-0.86 \pm 0.10}$ , similar to that found locally. The 1- $\sigma$  intrinsic scatter about this plane is  $\pm 14\%$  in  $M/L_V$ , comparable to that observed in Coma. We conclude that even at intermediate redshifts, E and S0 galaxies are structurally mature and homogeneous, like those observed in nearby clusters. The  $M/L_V$  ratios of these early-type galaxies are offset from the Coma fundamental plane by  $\Delta \log M/L_V = -0.13 \pm 0.03$  ( $q_0 = 0.1$ ), indicative of mild luminosity evolution in the stellar populations in the CL1358+62 E and S0 galaxies. This level of evolution suggests a luminosity-weighted formation epoch for the stars of  $z > 1$ . The precise redshift depends on the initial mass function and on the cosmology. The scatter about the fundamental plane is consistent with that in the color-magnitude relation, indicating that the E/S0s have a scatter in luminosity-weighted ages of  $\lesssim 15\%$ .

We have also analyzed the  $M/L_V$  ratios of galaxies of type S0/a and later. These early-type spirals follow a different plane from the E and S0 galaxies:  $r_e \propto \sigma^{0.66 \pm 0.29} \langle I \rangle_e^{-0.64 \pm 0.06}$ , with a scatter that is twice as large as the scatter for the E/S0s. The difference in the tilt between the plane of the spirals and the plane of the E/S0s is shown to be due to a systematic correlation of velocity dispersion with residual from the plane of the early-type galaxies. These residuals also correlate with the residuals from the color-magnitude relation. Thus for the spirals in this cluster, as well as for the three E+A galaxies in the sample, we see a systematic variation in the luminosity-weighted mean properties of the stellar populations with central velocity dispersion. If this is a relative age trend, then luminosity-weighted age is positively correlated with  $\sigma$ , *i.e.*, more massive spiral galaxies have older stars on average.

The residuals from the color-magnitude relation were used to correct the surface brightnesses of the early-type spirals. After this correction for age effects, these spirals fall on the fundamental plane of E/S0s. We conclude that the early-type spirals may well evolve onto the scaling relations of the old cluster members. After correcting the spirals for the systematic trend with color, their scatter about the fundamental plane does not decrease and remains twice as large as that for the E/S0s. This large scatter should be seen in a subsample of present-day cluster galaxies, if these spirals evolve into contemporary S0s, unless some unknown process reduces their scatter.

The colors and  $M/L_V$  ratios imply that many cluster galaxies were forming stars at least up until  $z \sim 0.5$ , but that this activity was specific to the spiral population. The E+As will likely evolve into low-mass present day S0 and Sa galaxies, but slightly bluer than the present-day ( $B - V$ ) color-magnitude relation by  $\sim 0.08$  mag, while fading to  $\sim 1$  mag below  $L^*$ .

*Subject headings:* galaxies: evolution, galaxies: elliptical and lenticular, galaxies: structure of, galaxies: clusters: individual (CL1358+62)

## 1. INTRODUCTION

For many years, the evolution of galaxies has been estimated through the use of galaxy counts (see the review by Koo & Kron 1992), and, more recently, using luminosity functions (*e.g.*, Lilly *et al.* 1995). However, such data do not uniquely constrain the luminosity evolution because of the unknown distribution of galaxy masses in a given sample, since  $M/L$  varies greatly with

star-formation history. Measurements of the mass scales of distant galaxies can remove this ambiguity by allowing one to observe  $M/L$  ratios and provide a direct, unambiguous measure of the luminosity evolution. Reliable estimates of the mass scales of galaxies at high redshifts can routinely be made using the high spatial resolution imaging cameras on the *Hubble Space Telescope* (HST), and efficient ground-based spectrographs on 8-10m telescopes. HST data provide the requisite length scales,

<sup>1</sup>Based on observations obtained at the W. M. Keck Observatory, which is operated jointly by the California Institute of Technology and the University of California.

<sup>2</sup>Based on observations with the NASA/ESA *Hubble Space Telescope*, obtained at the Space Telescope Science Institute, which is operated by AURA, Inc., under NASA contract NAS 5-26555.

<sup>3</sup>Department of Terrestrial Magnetism, Carnegie Institution of Washington, 5241 Broad Branch Rd., NW, Washington, DC 20015

<sup>4</sup>University of California Observatories / Lick Observatory, Board of Studies in Astronomy and Astrophysics, University of California, Santa Cruz, CA 95064

<sup>5</sup>Kapteyn Astronomical Institute, P.O. Box 800, NL-9700 AV, Groningen, The Netherlands

<sup>6</sup>Leiden Observatory, P.O. Box 9513, NL-2300 RA, Leiden, The Netherlands

and the spectrographs on 8-10m telescopes enable us to accurately measure internal kinematics. Together, one can directly measure  $M/L$  ratios through the use of galaxy scaling relations in a manner consistent with previous work on large samples of nearby galaxies. These scaling relations, such as the Tully-Fisher relation for spirals (Tully & Fisher 1977), the Faber-Jackson relation for ellipticals (Faber & Jackson 1976), or the fundamental plane of early-type galaxies (Faber *et al.* 1987, Djorgovski & Davis 1987), are essentially relations between  $M/L$  ratio and galaxy mass. Using such relations, one can directly probe the evolution of  $M/L$  ratios for galaxies at high redshift, and set powerful constraints on the evolution and formation histories of normal galaxies.

The fundamental plane (FP) is an empirical relation between half-light radius,  $r_e$ , surface brightness,  $\langle I \rangle_e$ , and central velocity dispersion,  $\sigma$  for early-type galaxies (Faber *et al.* 1987, Djorgovski & Davis 1987). The FP is a refinement of the Faber-Jackson relation. Using a large sample of E and S0 galaxies in 11 clusters, Jørgensen, Franx, & Kjærgaard (1996) found, for 226 galaxies in Gunn  $r$  and 109 in Gunn  $g$ ,

$$r_e \propto \sigma^{1.24 \pm 0.07} \langle I \rangle_e^{-0.82 \pm 0.02}, \quad (\text{Gunn } r) \quad (1)$$

$$r_e \propto \sigma^{1.16 \pm 0.10} \langle I \rangle_e^{-0.76 \pm 0.04}, \quad (\text{Gunn } g) \quad (2)$$

Under the assumption of homology, the FP implies that  $M/L$  ratio is a tight function of galaxy structural parameters, such that, in Gunn  $r$ ,

$$M/L_r \propto M^{1/4} r_e^{-0.02} \quad (3)$$

(Faber *et al.* 1987). The fundamental plane is very thin (Lucey, Bower, & Ellis 1991), with an observed *rms* scatter of  $\pm 20\%$  in Coma in  $V$ -band  $M/L$  ratio at a given  $M$  (Jørgensen, Franx, & Kjærgaard 1993).

By measuring a large sample of early-type galaxies at high redshift (*i.e.*, at large look-back time), one can use the evolution of  $M/L$  ratios and the evolution of the scatter in  $M/L$  to infer the star-formation histories of early-type galaxies. In this way, one directly measures the star-formation history of the Universe in high-density regions (where early-type galaxies are predominantly found, *e.g.*, Dressler 1980). Franx (1993, 1995) and van Dokkum & Franx (1996) used the MMT to obtain spectroscopy of several early-type galaxies in the clusters A665 ( $z = 0.18$ ) and CL0024+16 ( $z = 0.39$ ). They used structural parameters from HST imaging, and velocity dispersions from the spectroscopy, to derive  $M/L$  ratios for early-type galaxies in those clusters. Due to the low internal scatter in the fundamental plane, even these few observations sufficed to measure mild evolution in the  $M/L$  ratios as a function of redshift. Several other authors have now measured elliptical galaxy scaling relations at intermediate redshifts and have confirmed mild (passive) stellar evolution out to moderate redshifts ( $z \lesssim 1$ ; Schade *et al.* 1997, Ziegler & Bender 1997, Pahre 1998).

Kelson *et al.* (1997) extended the fundamental plane measurements to CL1358+62 ( $z = 0.33$ ) and MS2053-04 ( $z = 0.58$ ) and confirmed the moderate  $M/L$  evolution. Those authors also suggested that the evolution in the scatter is likely to be quite low. Here, we present the analysis of a larger sample of more than 50 galaxies in CL1358+62 at  $z = 0.33$ . The spectroscopy and surface photometry are discussed by Kelson *et al.* (1999a,b). Using these data, we now analyze the fundamental plane in the cluster, with the goal of addressing the following issues:

(1) What is the form of the fundamental plane at high redshift? Does the slope evolve with redshift? What is the scatter,

and does it evolve with redshift? Is there simply a  $M/L$  zero-point shift?

(2) Is there any *morphological* dependence in the fundamental plane at high redshift, since large, nearby samples show no obvious dependence or difference between S0s and ellipticals (Jørgensen, Franx, & Kjærgaard 1996)?

(3) Do  $M/L_V$  ratios, for a given galaxy mass, correlate with known stellar population indicators, such as  $(B-V)$  color, or with structural indicators, such as apparent ellipticity or profile shape?

(4) How do “E+A” galaxies relate to the typical early-type cluster members? E+A galaxies have spectra which appear to be superpositions of an old early-type stellar population, and a young 1-2 Gyr-old stellar population (Dressler & Gunn 1983). Do these E+A galaxies have any immediate connection to the present-day S0 population (Franx 1993)?

This paper is structured as follows. In §2, we outline the selection and nature of the sample. In §3, the fundamental plane of the early-type galaxies is fit to the data, the S0s are compared to the ellipticals, and the intrinsic scatter about the fundamental plane is measured. In §4, we discuss the early-type galaxy  $M/L_V$  ratios and their implications for the stellar populations. In particular, we derive the evolution in  $M/L_V$  with respect to the early-types in Coma; derive the extent to which stellar populations are varying along the fundamental plane; and determine the nature of the scatter in the fundamental plane and color-magnitude relations. In §5, the fundamental plane of the early-type spirals is discussed, and their  $M/L_V$  ratios are compared to those of the E/S0s. In §6, population synthesis models are used to investigate the differences between the stellar populations of the spirals and early-types, with the goal of determining whether or not intermediate redshift spirals can evolve into contemporary S0s. Our conclusions will be summarized in §7.

## 2. SUMMARY OF SAMPLE SELECTION, OBSERVATIONS, AND DATA REDUCTION

We are currently studying the galaxy populations of three clusters in detail, CL1358+62 ( $z = 0.33$ ), MS2053-04 ( $z = 0.58$ ), and MS1054-03 ( $z = 0.83$ ), selected from the Einstein Medium Sensitivity Survey (Gioia *et al.* 1992). During Cycle 5, a mosaic of twelve HST WFPC2 pointings of CL1358+62 was taken in two filters, F606W and F814W. These data were presented in van Dokkum *et al.* (1998a).

A large number of redshifts in the cluster has been compiled by Fisher *et al.* (1998), who defined membership between  $0.31461 < z < 0.34201$ . Using 232 cluster members within a  $10' \times 11'$  field of view, they found a velocity dispersion for the cluster of  $1027^{+51}_{-45} \text{ km s}^{-1}$  (See Fisher *et al.* (1998) and Fabricant *et al.* (1999) for discussions about the spatial and kinematic distributions broken down by spectroscopic and morphological classifications). For fundamental plane analysis, we randomly selected cluster members within the field of view of the HST mosaic, to  $R \leq 21$  mag. The selection was performed with an effort to efficiently construct multi-slit plates for the Low-Resolution Imaging Spectrograph (Oke *et al.* 1995). We used three masks, with different position angles on the sky. The region of maximum overlap is in the center of the cluster, and thus the FP sample is concentrated towards the core of the cluster.

Morphology was not a factor in the selection of our sample. In the random selection process, three E+A galaxies were included; these will be compared with those cluster members that have normal, early-type spectra. The sample is about 50% complete for  $R \leq 20.5$  mag (see Fisher *et al.* 1998 for details on the

statistical completeness of the original redshift catalog). Three galaxies fainter than  $R = 21$  mag were added to test the quality of velocity dispersion measurements at faint magnitude limits.

The spectroscopic reductions are detailed in Kelson *et al.* (1999a). In total, we have central velocity dispersions for 55 galaxies in the cluster. Kelson *et al.* measured central velocity dispersions within an approximately  $1'' \times 1''$  aperture and corrected the values for aperture size to a nominal circular aperture of  $D = 3''.4$  at the distance of Coma. Kelson *et al.* (1999a) also showed that the kinematic profiles of the CL1358+62 members are similar to nearby early-type galaxies, ensuring that the aperture corrections derived from nearby galaxies remain valid for the  $z = 0.33$  data. Furthermore, the E/S0s and early-type spirals have similar kinematic profiles, over the aperture that Kelson *et al.* (1999a) used, ensuring that the velocity dispersion aperture corrections do not depend strongly on morphology.

The derivation of structural parameters from the HST imaging is discussed in Kelson *et al.* (1999b). Unfortunately, two of the galaxies were imaged too close to the WFPC2 CCD edges to obtain reliable structural parameters. Thus, there are a total of 53 cluster members in our determination of the fundamental plane in CL1358+62.

As was mentioned earlier, three galaxies have E+A spectra as defined by the criterion of Fisher *et al.* (1998), in which  $(H\delta + H\gamma + H\beta)/3 > 4 \text{ \AA}$  and  $[\text{OII}] 3727 \text{ \AA} < 5 \text{ \AA}$ . The E+A fraction of our sample (6%) is representative of the cluster (5%; Fisher *et al.* 1998). Two of the 53 galaxies show evidence of current star formation activity, with Balmer and [OIII] emission (the cD, #375; and the Sb, #234). Fisher *et al.* (1998) report an emission-line galaxy fraction of  $9 \pm 3\%$  in the field of the HST mosaic down to  $R = 21$  mag. In the sample presented here, the fraction is about half that (a  $2\sigma$  difference), though the emission-line galaxies are more common in the outer parts of the cluster. Although the cD shows evidence for emission in its central parts, we consider it “normal” and spectroscopically early-type for the fundamental plane.

Optical morphologies have been taken from Fabricant *et al.* (1999). These authors classified several hundred galaxies in the HST mosaic according to morphological type,  $T$ . The galaxies in our high-resolution spectroscopic sample have  $T \in \{-5, -4, -3, 0, 1, 2, 3\}$  (E, E/S0, S0, S0/a, Sa, Sab, Sb, respectively). The galaxy morphologies are listed in Table 1, in which there are 11 Es, 6 E/S0s, 14 S0s, 13 S0/as, 6 Sas, 2 Sabs, and 1 Sb. This distribution is quite similar to nearby massive clusters (*e.g.*, Oemler 1974). Note that the classification scheme employed in Fabricant *et al.* (1999) is not identical to that applied in van Dokkum *et al.* (1998a). The latter authors classified galaxies based on whether or not they had any obvious disk structure, and did not attempt to classify their galaxies according to the traditional Hubble scheme.

The photometric parameters were derived from the deep WFPC2 data. The surface photometry was transformed to Johnson  $V$ , redshifted to the frame of the galaxies. Such a transformation is necessary to facilitate a direct comparison of our sample with nearby galaxies. Details of the transformation are given in van Dokkum & Franx (1996) and Kelson *et al.* (1999b). The formal uncertainties in the individual structural parameters do not fairly represent the true errors in the fundamental plane determination. Random and systematic errors in  $r_e$  and  $\langle \mu_e \rangle$  can be quite large, but their combined error in the fundamental plane is quite small, at the level of a few percent (see Kelson *et al.* 1999b and, for example, the detailed analysis presented in

Saglia *et al.* 1997). The structural parameters were derived using three different profiles: (1) the de Vaucouleurs  $r^{1/4}$ -law; (2) generalized  $r^{1/n}$ -laws (Sersic 1968); and (3)  $r^{1/4}$ -law bulge plus exponential disk superpositions. Therefore, for each galaxy we have three sets of structural parameters. In §3.3 and 5.1, we investigate the utility of these different profiles, for purposes of morphological classification, or for determining accurate half-light radii and surface brightnesses.

The galaxy parameters used in the following analysis are listed in Table 1. Included are the optical morphologies, the  $n$  shape parameters, central velocity dispersions,  $r_e$  and  $\mu_e$  from the  $r^{1/4}$ -law fit,  $R$  magnitude from Fabricant *et al.* (1991), and restframe  $(B-V)$  colors from van Dokkum *et al.* (1998a). All three, different sets of structural parameters are listed in Kelson *et al.* (1999b). They are not critical for the conclusions of this paper.

### 3. THE FUNDAMENTAL PLANE OF EARLY-TYPE GALAXIES

#### 3.1. Fitting the Fundamental Plane

The fundamental plane is a power-law relation between effective radius,  $r_e$ , central velocity dispersion,  $\sigma$ , and mean surface brightness,  $\langle I \rangle_e$ , within  $r_e$ , of the following form:

$$\log r_e = \alpha \log \sigma + \beta \log \langle I \rangle_e + \gamma. \quad (4)$$

For the present analysis, we follow the procedures of Jørgensen *et al.* (1996), who found the best-fit plane through the data by minimizing the average absolute residual, perpendicular to the fitted plane. This method has the advantage of being robust against outliers. Similar to minimizing  $\chi^2$  using a gradient search algorithm, we search the parameter space of  $\alpha$  and  $\beta$  for the values which minimize

$$\chi = \sum \frac{|\log r_e - (\alpha \log \sigma + \beta \log \langle I \rangle_e + \gamma)|}{\sqrt{1 + \alpha^2 + \beta^2}} \quad (5)$$

$$= \sum \frac{|\Delta \log r_e|}{\sqrt{1 + \alpha^2 + \beta^2}} \quad (6)$$

where the denominator arises from the rotation of the residuals in  $\log r_e$  to a vector normal to the plane. This choice is also motivated, in part, by our desire to compare our results to the extensive work by Jørgensen *et al.*. In the fitting of a plane to three dimensional data, with correlated and uncorrelated errors, no single fitting procedure will accurately recover the underlying relation. An accurate determination of the true physical relation requires sophisticated modeling and knowledge of the underlying distribution of galaxy parameters, all of which are beyond the scope of this paper (Colless *et al.* 1999, Kelson 1999). As was mentioned earlier, Jørgensen *et al.* (1996) found  $\alpha = 1.16 \pm 0.10$ ,  $\beta = -0.76 \pm 0.04$  in Gunn  $g$  using 109 galaxies in nearby clusters. We adopt these values for the local slope of the fundamental plane, as Gunn  $g$  more closely matches the Johnson  $V$ -band, than does Gunn  $r$ . Nevertheless, one should note that the slopes for the local fundamental plane do not differ greatly between the two bandpasses and our conclusions in this paper are not sensitive to this choice.

Uncertainties in the values of  $\alpha$ ,  $\beta$ , and  $\gamma$  are estimated by the bootstrap method (*e.g.*, Beers, Flynn, & Gebhardt 1990). Such uncertainties represent the formal errors in the fit, when performed in the manner we have adopted (minimizing the absolute residuals). Systematic errors in the coefficients of the fundamental plane can arise from many sources, such as the selection criteria, the correlated measurement errors, and the choice

of the fitting procedure itself (*e.g.*, Jørgensen, Franx, & Kjærgaard 1996, Kelson 1999). For example, differences in fitting techniques can lead to small changes in the coefficients on the order of  $\pm 0.1$  or so. Thus, the fitting procedures of Jørgensen *et al.* (1996) were adopted partly so that this systematic effect would be minimized in our measurement of evolution in the coefficients. The systematic effects arising from selection biases and correlated measurement errors are still being explored, and will be published later (Kelson 1999).

The scatter about the best-fit plane will be reported either in units of  $r_e$  at fixed  $\sigma$  and  $\langle I \rangle_e$ , or in units of  $M/L_V$  at fixed  $\sigma$  and  $r_e$ . Under the assumption of homology, the observed quantities  $r_e$ ,  $\langle I \rangle_e$ , and  $\sigma$  relate to real physical properties of size, surface brightness, and total second velocity moment, in the same manner for all early-type galaxies. Thus, one can use the fundamental plane of the ellipticals to transform the virial theorem

$$M/L|_{\text{obs}} \propto \sigma^2 r^{-1} \langle I \rangle_e \quad (7)$$

into

$$M/L|_{\text{pred}} \propto \sigma^{\alpha/\beta+2} r_e^{-(1+\beta)/\beta} \quad (8)$$

In Gunn  $g$  the slopes for early-type galaxies of Jørgensen *et al.* (1996) yield  $M/L_g|_{\text{pred}} \propto \sigma^{0.47 \pm 0.15} r_e^{0.32 \pm 0.07}$

These equations enable us to express the fundamental plane residuals in units of  $M/L$  ratio:

$$\begin{aligned} \Delta \log M/L &= \log M/L|_{\text{obs}} - \log M/L|_{\text{pred}} \\ &= (\log r_e - \alpha \log \sigma - \beta \log \langle I \rangle_e - \gamma)/\beta \\ &= (\Delta \log r_e)/\beta \end{aligned} \quad (9)$$

Because the absolute residuals have been minimized, the *rms* scatter about any given fit is not. We therefore refrain from writing the scatter as an *rms* value, and instead report estimates of the  $1-\sigma$  scatter using  $1.25 \times$  the average absolute deviation, either in  $r_e$  or in  $M/L_V$ . For a Gaussian distribution of residuals, this estimate for the scatter is equivalent to the standard deviation. We find similar results when using the bi-weight statistic (Beers, Flynn, & Gebhardt 1990), and conclude that our estimate of the scatter is robust.

In constructing the figures, we express  $r_e$  in units of kpc, and  $\langle I \rangle_e$ , the mean surface brightness within an effective radius, in units of  $L_\odot/\text{pc}^2$  in the  $V$ -band. For the purposes of this paper, we use  $H_0 = 65 \text{ km s}^{-1} \text{Mpc}^{-1}$  and  $q_0 = 0.1$ , defining a scale of 4.8 kpc/arcsec.

### 3.2. The Fundamental Plane in CL1358+62

In Figure 1, we show the fundamental plane of early-type galaxies. The long, intermediate, short edge-on projections, and the face-on projection are shown in Fig. 1(a-d). There is a tight relation, offset from the relation defined by the early-type galaxies of Coma (Jørgensen, Franx, & Kjærgaard 1996). In 1(d), the “Zone of Avoidance” (Bender, Burstein, & Faber 1993) is the region in the upper right which contains no galaxies. Note that the CL1358+62 early-type galaxies have a different distribution than the Coma galaxies: the CL1358+62 galaxies lie at slightly higher surface brightnesses. We will come back to this point later.

The fundamental plane of the 30 E, E/S0, and S0 galaxies (not including any galaxies with E+A spectra) is described by

$$r_e \propto \sigma^{1.31 \pm 0.13} \langle I \rangle_e^{-0.86 \pm 0.10} \quad (10)$$

The  $1-\sigma$  scatter is only  $\pm 14\%$  in  $r_e$ . Using Equation 9, one obtains

$$M/L_V|_{\text{pred}} \propto \sigma^{0.48 \pm 0.18} r_e^{0.16 \pm 0.14} \quad (11)$$

with a scatter of about  $\pm 16\%$  in  $M/L_V$  ratio. The scatter in  $M/L_V$  is 18% when using the locally defined Gunn  $g$  slopes.

The values obtained above for the slope do not significantly differ from that found locally, either in Gunn  $g$  or Gunn  $r$  (see above). Comparing Equation 11 to the local expectation in Gunn  $g$ , one finds that the slope of the fundamental plane has not significantly evolved from the present-day:

$$\begin{aligned} \log M/L|_{z=0.33} - \log M/L|_{z=0} &\propto \\ (0.01 \pm 0.23) \log \sigma - (0.16 \pm 0.16) \log r_e \end{aligned} \quad (12)$$

Both van Dokkum & Franx (1996) and Kelson *et al.* (1997) noted that the intermediate redshift FP slope may not be the same as that found locally. The advantage of the work presented here is the depth and size of the sample, which allows for a more detailed breakdown by morphological type. Kelson (1998, 1999) show that a shallow magnitude cut-off in the selection process can lead to a flattening of the fitted fundamental plane slope, similar to other Malmquist-like regression biases. Such an effect probably led to the mild change in slope observed by Kelson *et al.* (1997) and van Dokkum & Franx (1996).

### 3.3. Quantitative Morphologies

We tested the robustness of the slope to the morphological classifications. Using the Sersic (1968) profile shape parameters  $n$  as a classification tool, the plane of the 30 galaxies with  $n \geq 4$  are best fit by  $\alpha = 1.19 \pm 0.23$  and  $\beta = -0.76 \pm 0.12$ . Using the 1D bulge-disk decompositions, the plane of the 25 galaxies with bulge fractions greater than 90% are best fit by  $\alpha = 1.19 \pm 0.17$  and  $\beta = -0.76 \pm 0.06$ . Recall that the visually classified E/S0s galaxies produced slopes of  $\alpha = 1.31 \pm 0.13$  and  $\beta = -0.86 \pm 0.10$ . We conclude that our measured fundamental plane slopes are not affected by uncertainties in the morphological classifications.

Since the slopes we have determined for the CL1358+62 FP do not differ significantly from that found by Jørgensen *et al.* (1996), as given earlier, we continue our analysis using the locally defined values of  $\alpha = 1.16$  and  $\beta = 0.76$ . The remaining conclusions of this paper are not sensitive to the adoption of these values over the ones measured above.

### 3.4. Elliptical Galaxies versus Lenticulars

For nearby S0s, the zero-point and scatter of the fundamental plane is the same as that for ellipticals (Jørgensen, Franx, & Kjærgaard 1996). Using either the fundamental plane coefficients defined by the 30 CL1358+62 early-types, or the ones defined locally, the 11 ellipticals have the same zero-point as the 13 non-E+A S0s. This is fully consistent with what has been found in nearby clusters.

There remains, however, the question of whether the slope of the fundamental plane of the S0s is the same as that of the ellipticals. The 11 visually classified ellipticals yield  $\alpha = 1.25 \pm 0.26$  and  $\beta = -0.71 \pm 0.16$  with a  $1-\sigma$  scatter of  $\pm 10\%$  in  $r_e$ . There appears to be no significant change in the slope by removing the one elliptical fainter than the magnitude limit and exclusion of the cD does not significantly affect the slope either. By fitting a plane to the 13 non-E+A S0s in CL1358+62, we

find  $\alpha = 1.12 \pm 0.36$ ,  $\beta = -0.86 \pm 0.22$ , with a scatter of  $\pm 8\%$ . The difference in scatter is not statistically significant. Because the distinction between E and S0 can become more difficult at higher redshift, we have also divided the sample of 53 galaxies by bulge-to-disk ratio, derived from fitting two-component  $r^{1/4}$ -law bulge and disk growth curves to surface photometry (Kelson *et al.* 1999b). No significant difference in the fundamental plane slopes are seen for any of these subsets.

As a result of these tests, we conclude that differences between the coefficients of the FP relations of the S0s and Es, if any, are too subtle to be accurately measured with the current sample.

### 3.5. The Intrinsic Scatter of the Early-Type Galaxies

In cosmological models involving hierarchical merging of gas-rich systems, early-type galaxies are expected to have some intrinsic scatter in the properties of their stellar populations (Kauffmann 1995, 1996). Such variations would manifest themselves in a scatter in the colors, absorption line strengths, and  $M/L_V$  ratios of early-type galaxies at a given luminosity, galaxy mass, or velocity dispersion (Sandage & Visvanathan 1978, Terlevich *et al.* 1981, Faber *et al.* 1987).

Evidence for a spread in the properties of stellar populations has been measured using the scatter about the color-magnitude relation (e.g., Bower, Lucey, & Ellis 1992, Ellis *et al.* 1997, Stanford, Eisenhardt, & Dickinson 1998). We have measured the scatter in colors about the color-magnitude relation for the galaxies in our sample and find an *intrinsic*  $1-\sigma$  scatter in color, at a given mass, of  $\pm 0.018$  mag (see van Dokkum *et al.* 1998a). Using the GISSEL96 (Leitherer *et al.* 1996) single burst stellar populations with a Salpeter (1955) initial mass function (IMF), and assuming that variations in age are the cause of these residuals, this scatter in color is equivalent to a scatter in  $M/L_V$  of  $\pm 13\%$ .

Equation 9 showed that variations in  $M/L_V$  ratios of stellar populations, at a given  $r_e$  and  $\sigma$  will lead to scatter in the fundamental plane. Residuals from the fundamental plane can be caused by a number of other effects as well, such as variations in elliptical galaxy shapes, metal abundance, and dust content. In contrast, the scatter in the color-magnitude relation may only be due to variations in stellar populations and/or dust content. Some have also suggested that correlations between age, other stellar population properties, and/or galaxy structural parameters may be conspiring to reduce the scatter in the fundamental plane and color-magnitude relations (cf. Worthey, Trager, & Faber 1996, Trager *et al.* 1999). Jørgensen *et al.* (1996) have limited to what extent random projection can inflate the scatter of the fundamental plane to less than 6% in  $M/L$  ratio. Together, the scatter in the fundamental plane and color-magnitude relations can be used to constrain the properties of the stellar populations.

The ellipticals and S0s have an observed  $1-\sigma$  scatter about the FP of  $\pm 16\%$  in  $M/L_V$ . The observational errors in our data are a small component of the observed scatter. As shown in Kelson *et al.* (1999a), the formal velocity dispersion uncertainties range from  $\pm 2$ -7%. Because of template mismatch, the true errors are more like  $\pm 4$ -8%. The fundamental plane parameters,  $r_e \langle I \rangle_e^{-0.8}$ , have random errors of  $\pm 3\%$  (Kelson *et al.* 1999b). Thus, the contribution to the observed scatter from measurement errors is approximately  $\pm 7\%$  in  $r_e$  ( $\pm 8\%$  in  $M/L_V$ ). Removing this in quadrature gives an intrinsic scatter in  $M/L_V$  of  $\pm 14\%$ . That the intrinsic scatter in  $M/L_V$  should agree so well with the naive expectation from the scatter in colors is remarkable. Moreover,

the intrinsic scatter of 14% is an upper limit to the scatter in the stellar populations because there may be other sources of scatter in the observed  $M/L_V$  ratios, due to variations, for example, in galactic structure.

## 4. IMPLICATIONS FOR THE STELLAR POPULATIONS OF EARLY-TYPE GALAXIES

### 4.1. The Evolution of the Zero-point for the Fundamental Plane of Early-Type Galaxies

The zero-point of the fundamental plane is related to the mean  $M/L$  ratio of a sample of early-type galaxies. Evolution in the luminosity-weighted mean properties of stellar populations therefore implies evolution in the FP zero-point. Although modest evolution of the FP zero-point has already been demonstrated (van Dokkum & Franx 1996, Kelson *et al.* 1997, van Dokkum *et al.* 1998b), these new data can improve upon the accuracy of the results in Kelson *et al.*, and test the sensitivity to small number statistics and sample biases.

We use a sample of early-type galaxies in Coma to define the present-day zero-point of the fundamental plane. These data are a subset of the large Gunn *r* sample in Jørgensen *et al.* (1996) that also had the required color information to transform the surface brightnesses to the *V*-band. This *V*-band Coma sample is shown in Figures 1(a-d) by the small triangles. Note that the CL1358+62 early-types are shifted by a small amount with respect to the Coma early-types. The trend appears to be towards increasing surface brightnesses, suggesting that at least some of the shift in  $M/L$  derives from luminosity evolution.

If the ranges of galaxy masses in Coma and CL1358+62 are substantially different, which was the case for the small samples in van Dokkum & Franx (1996), Kelson *et al.* (1997) and van Dokkum *et al.* (1998b), then the offset in  $M/L_V$  can be very sensitive to the adopted slopes of the fundamental plane. This sensitivity arises because the fundamental plane is essentially a relation between  $M/L_V$  ratio and galaxy mass. If one compares two samples of galaxies with substantially different mass functions, then any derived offset in  $M/L_V$  is going to be a combination of the true offset, the differences in FP slope, and the difference in the mean mass of the sample. By minimizing the differences between the mass distributions, one eliminates this latter term, and the results become insensitive to the slope of the FP. Therefore, when deriving the offsets, we restrict the local calibrating sample to a similar mass range as in CL1358+62. Such a restriction on the local sample implies that any measured evolution is relevant for galaxies within a specific range of masses.

In Figure 2, we show the distributions of the CL1358+62 galaxies overlaid with the Coma *V*-band sample in the  $\log \sigma$ - $\log r_e$  plane. The dashed lines show contours of constant mass ( $5G^{-1}\sigma^2 r_e = 10^{10,11,12} M_\odot$ , Bender, Burstein, & Faber 1992). The distributions are remarkably similar, ensuring that our measurement of the  $M/L_V$  evolution will not be biased by any differences between the two distributions of galaxy masses.

Using the 30 early-type galaxies, we find that the  $M/L_V$  ratios, for a given  $r_e$  and  $\sigma$ , are offset by  $\Delta \log M/L_V = -0.13 \pm 0.03$  ( $q_0 = 0.1$ ;  $-0.10 \pm 0.03$  dex for  $q_0 = 0.5$ ). The errors listed are the formal errors in the offset. We test the sensitivity of this result to the morphological classifications by using only the Es and find no significant difference. Changing the adopted slope from the Jørgensen *et al.* (1996) Gunn *g* values to those for Gunn *r* changes the results by  $-0.02$  dex. Using the values found in §3 also produces no significant

change in the result as well. Kelson *et al.* (1997) had found  $\Delta \log M/L_V = -0.17 \pm 0.05$  dex. The difference can be attributed to improvements in the size and depth of the sample.

We can use the simple, single-burst models of §6 to infer the relative age difference between the Coma and CL1358+62 early-types. Assuming that the early-type galaxies in both clusters have had similar formation histories and adopting a Salpeter IMF, the CL1358+62 early-type galaxies have ages in the mean which are  $70 \pm 5\%$  ( $q_0 = 0.1$ ;  $76 \pm 5\%$  for  $q_0 = 0.5$ ) of the mean ages of their counterparts in Coma, for galaxies of the same  $r_e$  and  $\sigma$ . These uncertainties are the internal errors alone. The external errors account for another 5-10%. Thus,  $\sim 1/4$  of the lifetimes of cluster ellipticals has passed during the last 30% of the age of the universe.

#### 4.2. The Variation in $M/L_V$ along the Fundamental Plane

In the previous section we showed that the intrinsic scatter in the fundamental plane is very low, at  $\sim 14\%$  in  $M/L_V$  ratio. The implication is that the  $M/L_V$  ratios of E/SOs are very tightly correlated with their structural parameters in CL1358+62. In this section, we introduce simple models for stellar populations to address the implications of such a correlation.

Tinsley & Gunn (1976) first showed that the  $M/L_V$  ratio of a single-burst stellar population evolves as

$$M/L_V \propto t^{1.2-0.28x}, \quad (13)$$

where  $t$  is the time since the formation epoch, and  $x$  is the slope of the initial mass function. They found very little dependence on metallicity,  $Z$ . This model predicts  $\log M/L_V \propto 0.82 \log t$  for an IMF with  $x = 1.35$  (Salpeter 1955). For composite stellar populations,  $t$  and  $Z$  are luminosity-weighted mean ages and metal abundances.

For our analysis, we turn to the GISSEL96 (Leitherer *et al.* 1996) stellar population synthesis models. We choose to use bivariate least-squares fits to the model curves in order to use simple analytical expressions in the analysis. The models of single-burst stellar populations older than  $t \geq 2$  Gyr, with a Salpeter (1955) IMF from  $m = 0.1-125M_\odot$  are well fit by

$$\log M/L_V = -6.74 + 0.84 \log t + 0.56 \log Z + 0.076(\log Z)^2, \quad (14)$$

and

$$(B-V) = -1.19 + 0.27 \log t + 0.34 \log Z + 0.027(\log Z)^2, \quad (15)$$

where  $t$  is in Gyr, and  $Z$  is the metal abundance (solar abundance ratios), between  $Z = 4 \times 10^{-4}$  to  $5 \times 10^{-2}$ . For composite stellar populations, the properties of age and metallicity are mean properties of the luminosity-weighted sum of the stellar populations within each galaxy.

The implication of Equations 14 and 15 is that  $M/L_V$  ratios should be correlated with galaxy color. This correlation is explicitly shown in Figure 3(a). Because the underlying correlations of  $M/L_V$  and  $(B-V)$  with  $r_e$  and  $\sigma$  have not been removed, the figure is a combined projection of the fundamental plane and color-magnitude relations. A Spearman rank correlation test indicates a probability of 99.9% that the  $(B-V)$  colors and  $M/L_V$  ratios of the E/SOs are correlated.

A linear least-squares fit to the points in the figure gives  $\log M/L_V \propto (2.55 \pm 0.79) \times (B-V)$ , shown by the thick solid line. The shaded region indicates the  $\pm 1\sigma$  errors in the slope. The uncertainty in the slope is large because the scatter in the

diagram is large, and because the errors for individual measurements of  $M/L_V$  are also large.

As stated above, the time-evolution of  $M/L_V$  is governed largely by the shape of the IMF (Tinsley & Gunn 1976). For stellar populations of constant metallicity Equations 14 and 15 imply a relation between  $M/L_V$  ratio and color of  $\log M/L_V \propto 3.1 \times (B-V)$ . Thus, if the correlation in Figure 3(a) is the result of a systematic variation in galaxy age, then one would expect a slope indicated by the thin solid line. Under this assumption, any departure of the data in Figure 3(a) from a slope of 3.1 implies an error in the adopted IMF. Using the IMF dependence of Equation 13, we make the following simple modification to Eq. 14:

$$\log M/L_V = -6.74 + (1.22 - 0.28x) \log t + 0.56 \log Z + 0.076(\log Z)^2. \quad (16)$$

Equation 15 is insensitive to the shape of the IMF because the dependence of both the  $M/L_V$  and  $M/L_B$  ratios on  $x$  is nearly identical (Tinsley & Gunn 1976). Put another way,  $(B-V)$  color is related to the temperature of the main-sequence turn-off stars, which itself is independent of the shape of the IMF.

Using the least-squares fit to Figure 3(a), the slope of the IMF is constrained to be  $x = 1.9 \pm 0.8$ . The implication of this IMF is that  $M/L_V$  evolves according to  $\log M/L_V \propto (0.67 \pm 0.22) \log t$ . Given that  $\log M/L_V \propto 0.24 \log M + 0.08 \log r_e$ , one concludes  $\log t \propto \sim 0.35_{-0.08}^{+0.18} \log M$ . The implication is that the mean luminosity-weighted age of elliptical galaxies in CL1358+62 with  $\sigma = 100 \text{ km s}^{-1}$  is  $45_{-15}^{+8}\%$  of the mean luminosity-weighted age of the  $\sigma = 300 \text{ km s}^{-1}$  ellipticals. For a Salpeter (1955) IMF, this ratio of ages is 50%.

If a systematic trend in metallicity is causing the correlation in Figure 3(a), then, near solar metallicities, the slope should be  $\log M/L_V \sim 1.2(B-V)$ , shown by the thin dash-dot line. The fitted slope is discrepant from that expected from metallicity effects by less than  $2\sigma$ . Worthey (1994) and others have suggested that luminosity-weighted ages and metallicities are correlated such that  $\Delta \log t / \Delta \log Z \propto -3/2$ . The expected curve is based on this relation is shown as the thin dotted line in Figure 3(a). No particularly strong constraints can be made with the current data if both age and metallicity are varying.

The correlation of  $M/L_V$  ratio with  $(B-V)$  color can only be related to the stellar populations. Do these systematic variations in the stellar populations fully account for the observed slope of the fundamental plane? By correcting the surface brightnesses for the fitted correlation of  $M/L_V$  with  $(B-V)$  color, and fitting a new plane to the corrected data, we find:

$$\log r_e \propto (1.84 \pm 0.27) \log \sigma - (0.89 \pm 0.17) [\log \langle I \rangle_e + 2.55(B-V)] \quad (17)$$

This fit implies that the early-type galaxies in CL1358+62 are consistent with notion that they are a family of homologous objects. The uncertainties are large, in part, because we have assumed that the correlation between  $M/L_V$  ratio and  $(B-V)$  color applies for the entire sample of early-type galaxies in the cluster. Individual galaxies may have histories which deviate substantially from the mean star-formation history of E/SOs, and thus be poorly modeled by the fitted correlation. For example, we cannot assume that all early-type galaxies have constant metallicity at fixed age, or vice versa. There is some naturally occurring dispersion in the mean properties of the stellar populations of E/SOs and this dispersion is reflected as scatter in Figure 3(a).

More data, such as from absorption-line strengths and larger sample sizes, are required in order to reduce the uncertainties. Furthermore, more careful modeling of the observations will be required in order to fully account for the fitting biases and measurement errors (Kelson 1998, 1999).

#### 4.3. Understanding the Scatter in the FP and CM Relations

Residuals in the fundamental plane and color-magnitude relations are expected to be related through Equations 15 and 16. When the residuals in  $\log M/L_V$  and  $B-V$  are plotted against each other, as in Figure 3(b), no obvious correlation is seen for the E/S0s. Residuals from Eq. 17 do not show any significant correlation with the color-magnitude residuals either.

Perhaps measurement errors, or other sources of scatter besides the stellar populations are large enough to obscure any intrinsic correlation between the residuals from the relations? One source of uncertainty that has been ignored is the intrinsic correlation of  $r_e$  and  $\langle I \rangle_e$ , and how it propagates into errors in  $M/L_V$  ratio. The  $M/L$  ratios are expected to scale as  $(r_e \langle I \rangle_e)^{-1}$  for a homologous family of objects, yet the error correlation in the photometric structural parameters indicates a correlation of  $r_e \langle I \rangle_e^{-0.75}$  (Kelson *et al.* 1999b, Kelson *et al.* 1999c). Given the typical random uncertainties in half-light radii of approximately  $\delta \log r_e \approx 0.15$  dex, the corresponding, random uncertainties in  $M/L_V$  are  $\delta \log M/L_V \approx 0.05$  dex. This additional source of error does not have this large an impact on the fundamental plane scatter, however, because the underlying correlation between  $M/L_V$  and  $r_e$  is not orthogonal to the error correlation between  $r_e$  and  $\langle I \rangle_e$ . The error correlation is probably within  $\pm 30^\circ$  of the underlying correlation between  $M/L_V$  and  $r_e$  (Kelson 1999). Therefore the  $\pm 0.05$  dex random scatter in the  $M/L_V$  ratios is diminished in its contribution to the fundamental plane scatter. The effect of this error correlation is to mix up the distribution of galaxies within the fundamental plane, leaving correlations between  $\Delta \log M/L_V$  and  $\Delta(B-V)$  difficult to observe.

Because of the observational effects discussed in the previous paragraph, one's ability to interpret the scatter of the FP and CM relations is limited. While we cannot directly observe correlations between the FP and CM residuals, we can use the intrinsic scatter in the FP and CM relations to place constraints on the stellar populations. Several assumptions are made in the following analysis. In particular, we assume that the intrinsic scatter in both relations is due to a dispersion in the luminosity-weighted mean properties of the stellar populations at fixed  $r_e$  and  $\sigma$ .

The *intrinsic* scatters of the FP and CM relations were found to be  $\sigma_{\log M/L_V} = \pm 0.060 \pm 0.012$  dex, and  $\sigma_{(B-V)} = \pm 0.018 \pm 0.005$  mag. For the scatter in  $M/L_V$ , the observed value of is an upper limit for the stellar populations because the scatter we measure in  $M/L_V$  may in part be due to other factors, such as might be caused by random variations in galaxy shape.

We now assume that the scatter in colors is due solely to variations in stellar population ages, at fixed mass, and investigate the ramifications. The scatter in colors implies a 13% scatter in luminosity-weighted ages. Using the analytical models of the previous section, one expects

$$\Delta \log M/L_V \propto (4.52 \pm 1.0x) \times \Delta(B-V) \quad (18)$$

Using  $x = 1.35$ , the scatter in colors is equivalent to a 13% scatter in the  $M/L_V$  ratios.

The scatter in the two relations is remarkably consistent with a scatter in luminosity-weighted ages, at fixed mass. Using simple single-burst models of stellar populations, and assuming a

Gaussian distribution of residuals in  $\log M/L_V$ , we can draw some conclusions from the scatter in  $M/L_V$  and  $(B-V)$ . If the mean epoch of star-formation for cluster ellipticals is  $z = 2$ , then the  $1-\sigma$  scatter of 15% in the luminosity-weighted ages implies  $\pm 1-\sigma$  interval for the epochs of star-formation of  $1.4 \lesssim z \lesssim 3.5$ . The  $\pm 2-\sigma$  limits are  $1 \lesssim z \lesssim 9$ . Thus, 98% of the star-formation in ellipticals was finished by  $z \approx 1$ . These conclusions were based on an IMF of  $x = 1.35$ , a cosmology with  $q_0 = 0.1$ , and a mean formation redshift of  $z = 2$  that is independent of velocity dispersion.

By measuring the evolution of the scatter to higher redshifts, one can place stronger constraints on the star-formation rates and histories of cluster ellipticals and S0s. If there exist systematic variations in the mean luminosity-weighted ages of early-type galaxies along the fundamental plane, *e.g.*, §4.2), then one requires more detailed modeling to derive the star-formation histories (Kelson 1999).

#### 5. EXTENDING THE FUNDAMENTAL PLANE TO EARLY-TYPE SPIRALS

In §2, we stressed that morphological information was explicitly disregarded in selecting the spectroscopic sample discussed in this paper. In this section, we use the fundamental plane as a tool to place the later-type galaxies in the context of the evolution of cluster galaxies in general. By doing so, the cluster populations can be studied without biasing the results exclusively to the oldest elliptical and lenticular galaxies. This aspect of our program makes it unique among studies of high-redshift clusters (*e.g.*, Ellis *et al.* 1997, Ziegler & Bender 1997, Pahre 1998, Pahre, Djorgovski, & Carvalho 1998). We use the early-types in the comparison, as nearby fundamental plane data on spirals has not been collected in as systematic and homogeneous manner as has been for early-type samples.

In Figure 4, we expand the fundamental plane of early-types to include all 53 galaxies in the sample. Recall that the sample of 53 galaxies contains 22 galaxies of morphological type S0/a and later. It is clear from the figure that these early-type spirals show large scatter compared to the E/S0s (shown by the smaller symbols). Using all 53 galaxies, one obtains a plane with  $\alpha = 1.10 \pm 0.20$  and  $\beta = -0.83 \pm 0.08$ . These values of the slope are not significantly different than what was found earlier. Assuming that all of the galaxies are homologous, the  $1-\sigma$  scatter is equivalent to  $\pm 28\%$  in  $M/L_V$ . The scatter in the full sample is nearly twice as large as that of the early-types alone.

There are 22 galaxies classified as S0/a and later. These galaxies follow a fundamental plane with  $\alpha = 0.66 \pm 0.29$ ,  $\beta = -0.64 \pm 0.06$ , with a scatter of about  $\pm 32\%$  in  $M/L_V$ . This plane is a significant departure from that of the ellipticals. Excluding the E+As or the emission-line galaxy #234 does not affect the slopes or scatter significantly. This large scatter implies that the early-type spirals are very inhomogeneous compared to the E and S0 galaxies. By inhomogeneous, we refer to a dispersion in their observed  $M/L_V$  ratios at a given location along the FP. We can conclude that the large scatter seen in the full sample of galaxies is partly due to the inhomogeneity in the properties of the early-type spirals, and partly due to the fact that those galaxies follow a different plane than that of the E and S0 galaxies.

The difference in slope for the spirals, compared to the early-types, may have several sources: (1) additional rotational support, (2) systematic errors in their structural parameters, or (3) variations in their stellar populations. Any or all of these may

be in effect, but they must be correlated with the structural parameters in order for the fundamental plane of the spirals to be so well-defined. Inhomogeneities in any of these properties are likely to be present as well, given the large scatter shown above.

While we do expect  $M/L_V$  ratios, and thus the fundamental plane, to differ between elliptical and spiral galaxies, the assumption of homology may not be valid for our entire sample. For example, many of the galaxies show strong rotation (Kelson *et al.* 1999a), or large deviations from an  $r^{1/4}$ -law surface brightness profile.

### 5.1. The Spirals in the Context of the Early-Types

We have shown that spirals follow a fundamental plane which is systematically different from ellipticals and S0s. We now proceed to investigate whether this change in slope is due to structural (“non-homology”) or stellar population effects. In Figure 5 we show the residuals from the fundamental plane of the early-types plotted against (a) morphological type, (b) bulge fraction of total light,  $BF$ , (c) the Sersic (1968)  $n$  shape parameter, (d) apparent ellipticity,  $\epsilon$ , (e) velocity dispersion, and (f) residual from the color-magnitude relation,  $\Delta(B-V)$  (van Dokkum *et al.* 1998a). The figures show a clear trend of fundamental plane residual with galaxy morphology velocity dispersion, and with galaxy color as well.

There are two possibilities for the correlations seen in Figure 5. Perhaps there are inherent structural differences between the classes of E/S0s and early-type spiral galaxies, or perhaps the  $M/L_V$  ratios of the spirals deviate from the fundamental plane of the early-types because of stellar population differences. We now systematically determine which of these options is relevant for our data.

#### 5.1.1. Bulge-to-Disk Ratio

The figure shows a correlation with morphology, using  $T$ ,  $BF$ , and  $n$ . Early-type spirals clearly show large scatter, and systematically negative residuals. Galaxies with low bulge fraction of total light are also systematically offset from the galaxies with large bulge fractions. Using the Sersic (1968) profile shape parameter  $n$ , one finds that galaxies with low values of  $n$  have, on average, lower  $M/L_V$  ratios, for a given  $r_e$  and  $\sigma$ , and larger scatter in those  $M/L_V$  ratios, compared to galaxies with large values of  $n$ .

We tested whether using a pure  $r^{1/4}$ -law surface brightness profile to derive structural parameters might have caused the additional scatter and tilt for the FP of the spirals. Kelson *et al.* (1999b) derived several sets of structural parameters using  $r^{1/n}$ -law profiles and superpositions of an  $r^{1/4}$ -law bulge plus exponential disk. *Their results show that the combination of  $r_e$  and  $\langle I \rangle_e$  that enters the fundamental plane was very stable, irrespective of the choice of profile shape.*

By using the structural parameters derived from the  $r^{1/n}$ -law profiles, or bulge-plus-disk superpositions, we find no significant difference in the fundamental plane from that obtained earlier using the de Vaucouleurs structural parameters. Given the stability of the combination of  $r_e$  and  $\langle I \rangle_e$  that appears in the fundamental plane, as shown in Kelson *et al.* (1999b), we conclude that errors in the structural parameters are unlikely to have resulted in any inhomogeneities in the observed properties of the CL1358+62 sample. Therefore for the remainder of the paper, we exclusively use the de Vaucouleurs profile structural parameters.

#### 5.1.2. Projection

If differences in galactic structure are causing large, systematic residuals in  $M/L_V$  ratio with respect to the fundamental plane of the ellipticals, then one might expect to see a correlation with apparent ellipticity. Jørgensen *et al.* (1993, 1996) investigated correlations of ellipticity and  $c_4$  parameters with fundamental plane residuals in an effort to find additional parameters in the FP. They built realistic models of early-type galaxies and generated pseudo-observations of them. The data did not, however, follow any of the trends predicted by the pseudo-observations, despite having taken all of the observational procedures into account when making the models.

In Figure 5(d), we show the residuals as a function of apparent ellipticity. In the figure, we show the expected deviations in observed  $M/L_V$  ratio for pressure supported E2, E4 and E6 galaxies (solid lines), and for isotropic rotators of intrinsic flattening 0.6, 0.5, 0.4, 0.3, 0.2, and 0.15 (see, *e.g.*, Binney & Tremaine 1987, Saglia, Bender, & Dressler 1993). The data do not follow the predicted curves in any sensible way. For example the spirals do not behave as flattened rotators in this diagram, presumably because their residuals are dominated by stellar population effects (see below).

#### 5.1.3. Internal Kinematics

For the spiral galaxies in CL1358+62, Figure 5(e) shows that the residuals from the fundamental plane of the early-types is strongly correlated with central velocity dispersion. This correlation might suggest that central measurements of the velocity dispersion do not relate to the virial mass in the same way for the spirals as for the E/S0s. While it seems reasonable to expect that spiral galaxies are not homologous with E/S0s, Kelson *et al.* (1999a) showed that the rotation curves of the two families are similar, at least to radii of approximately  $2r_e$ , at the level of a few percent. We therefore conclude that systematic differences in the central  $M/L_V$  ratios of the two families of galaxies are not arising from structural effects.

#### 5.1.4. Stellar Populations

The other possibility is that the properties of the luminosity-weighted stellar populations are systematically varying as a function of  $\sigma$ , at a given  $r_e$ . Such a trend would suggest that the correlation in Figure 5(e), and the low value for  $\alpha$  for the spirals, may actually be rooted in a systematic variation of stellar populations with  $\sigma$ . This idea appears to be borne out by Figure 5(f), in which deviations from the fundamental plane are strongly correlated with residual from the color-magnitude relation, in a manner consistent with simple models of passive stellar evolution (shown as the dotted lines). The models overlayed in (f) are GISSEL96 models of single-burst stellar populations of different metallicities, all normalized to a formation epoch of  $z = 2$  ( $H_0 = 65 \text{ km s}^{-1} \text{Mpc}^{-1}$ ,  $q_0 = 0.1$ ). Thus, the lines are progressions of age (time since the burst) from the blue to the red.

Together, the correlations in (e) and (f) would produce a fundamental plane for the early-type spirals which has a different slope than the plane of the E/S0s.

#### 5.1.5. Environment

Studies of nearby galaxies have shown that position within a cluster is important for galaxy evolution (*e.g.* the morphology-density relation, Dressler 1980, Dressler *et al.* 1997). Our

cluster imaging covers  $\sim 1.5h^{-1}$  Mpc  $\times 1.5h^{-1}$  Mpc, well-suited for studies of the morphology-density relation at high redshift (Fabricant *et al.* 1999). Within our HST mosaic, the S0s and spirals do indeed appear more spatially extended than the ellipticals (van Dokkum *et al.* 1998a, Fabricant *et al.* 1999).

Given this trend and the result that the color-magnitude diagram is position dependent (van Dokkum *et al.* 1998a), one should expect a correlation between FP residual and distance from the cluster center. In Figures 6(a,b), we see that there is no *obvious* trend with clustercentric radius. The sample is too small and the uncertainties are simply too large to draw any conclusions with the current sample. More observations are required to determine the magnitude of any effect. The environmental dependence of the color-magnitude relation is seen in our sample in Figures 6(c,d) but it is not as obvious as in the full sample of van Dokkum *et al.* (1998a). As a reminder, those authors used nearly 200 galaxies in their analysis of the color-magnitude diagram of the cluster.

Let us now continue with a more in-depth discussion of the stellar populations.

## 6. MODELING THE STELLAR POPULATIONS OF THE EARLY-TYPE SPIRALS

In the previous section, we showed that the residuals of the spirals from the FP and CM relations are predominantly due to their stellar populations. Do the stellar populations of the spirals evolve differently than those in early-type galaxies? In §4 we introduced single-burst stellar population models which predicted that the  $M/L_V$  ratios themselves should be correlated with  $(B-V)$  color. In Figure 3(a), we showed that this prediction is consistent with the data for the early-type galaxies.

In Figure 7 we expand the plot of  $\log M/L_V$  as a function of galaxy color to include the entire sample. The least-squares fit to the E/S0s, given in §4, is shown by the thick solid line. As in the Figure 3(a), the  $1-\sigma$  uncertainties from that fitted slope are indicated by the shaded region. Single-burst stellar populations with a Salpeter (1955) IMF are expected to evolve along the thin solid line. In this diagram, we plot a quadratic approximation to the model because the linear, analytical expressions in §4 were not valid for extremely young stellar populations. The emission-free early-type spirals, including the E+A galaxies, are not inconsistent with the extrapolation of the E/S0s. A least-squares fit to the spirals which do not show emission or E+A spectra, *i.e.*, appear to be older than a few Gyr, yields a slope of  $\log M/L_V \propto (3.23 \pm 1.23)(B-V)$ , consistent with the slope found using the early-types. With larger samples and measurements of line strengths, one should be able to reduce the uncertainties and use such diagnostics to place constraints on composite stellar populations, or, for example, the universality of the IMF.

### 6.1. Age Effects

If the fundamental plane and color-magnitude residuals are due to differences in mean luminosity-weighted ages alone, recall that the model predicts  $\Delta \log M/L_V = (4.52 - 1.0x)\Delta(B-V)$ . If the IMF follows  $x = 1.35$  (Salpeter 1955), then the models give  $\Delta \log M/L_V \propto 3.1\Delta(B-V)$ . Also recall that the analytical expressions on which this approximation is based are only valid for stellar populations with ages greater than 2 Gyr. Thus, in order to test this prediction, we perform a least-squares fit to the residuals of those spirals with spectroscopically early-type spectra. This fit, which excludes the E+A galaxies and the star-forming, emission-line galaxy, gives  $\Delta \log M/L_V \propto$

$(2.32 \pm 0.65)\Delta(B-V)$ , shown as the dashed line in Figure 5(f). This fit implies an IMF slope of  $x = 2.0 \pm 0.8$ .

The spiral galaxies have clearly experienced more recent star-formation than the ellipticals and S0s. We would now like to correct for the differences in the ages of their stellar populations. Since we would like to use the E+A galaxies, which have stellar populations younger than 2 Gyr, we need a more appropriate analytical expression relating  $\Delta \log M/L_V = f[\Delta(B-V)]$ . In fitting a solar metallicity model, with a Salpeter (1955) IMF, between ages of 750 Myr and 8 Gyr, we find

$$\Delta \log M/L_V = 3.22[\Delta(B-V)]^2 + 3.26\Delta(B-V) \quad (19)$$

This quadratic is shown as the solid line in Figure 5(f). For galaxies with similar radial gradients in their stellar populations, only  $\langle I \rangle_e$  is directly affected by changes in  $M/L_V$  ratio. We therefore correct the surface brightnesses by

$$\langle I \rangle'_e = \langle I \rangle_e \times 10^{3.22[\Delta(B-V)]^2 + 3.26\Delta(B-V)}. \quad (20)$$

In fitting a new fundamental plane to the corrected spirals, we find  $\alpha' = 1.04 \pm 0.42$  and  $\beta' = -0.61 \pm 0.09$ , similar to the Jørgensen *et al.* (1996) values we adopted earlier, though with larger errors. The scatter about this evolved plane is still  $\sim 30\%$  in  $M/L_V$  ratio, leading to increased uncertainties in the fit. After correcting for color residuals, no further correlations of  $\Delta \log M/L_V$  with  $n$ ,  $BF$ , or  $\sigma$  are seen.

We conclude that after several Gyr, barring any further star-formation, or dynamical evolution (*i.e.*,  $r_e$  or  $\sigma$  do not change with time), these cluster spirals will fall on the fundamental plane of the E/S0s. In Figure 8, we show that the mass and length scales are comparable to the early-type sample, indicating that, once evolved, the early-type spirals would occupy similar locations on the fundamental plane as the E/S0s.

The scatter in the spirals, however, remains quite high compared to the E/S0s, at about 30% in  $M/L_V$  ratio. This high scatter may be attributed to a larger spread in possible more complex star-formation histories, to the greater role of dust in these galaxies, and possibly to the greater role of rotational support. An important question remains: does some mechanism transform the spirals into earlier morphological types while their stellar populations evolve? If such a transformation occurs, these early-type spirals may be the progenitors of some nearby S0 galaxies (see Kuntschner & Davies 1998). Given that Dressler *et al.* (1997) found reduced numbers of S0s and increased numbers of spirals in  $z = 0.55$  clusters, perhaps we are witnessing an early stage in the history and transformation of low-mass S0s.

### 6.2. The E+A Galaxies

For the S0/a and later-type galaxies,  $\Delta \log M/L_V$  was roughly proportional to  $\log \sigma$ . We interpret this as a correlation of the mean luminosity-weighted ages of early-type spirals with velocity dispersion (see §5.1):

$$\Delta \log t \sim (1.22 - 0.28x)^{-1} \log \sigma. \quad (21)$$

Therefore, for single-burst stellar populations, with a Salpeter (1955) IMF,  $\Delta \log t \sim 1.2 \log \sigma$ . The implication is that  $\sigma = 100 \text{ km s}^{-1}$  early-type spirals in clusters are  $\sim 1/4$  the luminosity-weighted ages of their  $\sigma = 300 \text{ km s}^{-1}$  counterparts. However, if there is a systematic variation of age along the fundamental plane of E/S0s, then this interpretation of the residuals may

only be a lower limit on the range of the luminosity-weighted ages of the cluster spirals.

The E+A galaxies are at the extreme end of this correlation of stellar populations and  $\sigma$ . Their  $M/L_V$  ratios are about  $-0.5$  dex too low to be consistent with an extrapolation of the fundamental plane of the ellipticals. Using the Salpeter (1955) IMF, we find that  $\Delta \log t \sim -0.6$ , which is equivalent to stating that the mean luminosity-weighted ages of the E+As in CL1358+62 are about  $1/4$  the mean luminosity-weighted age of the cluster ellipticals of the same  $r_e$  and  $\sigma$ . The implication is that these galaxies underwent their last burst of star-formation sometime between  $z = 0.4$  to  $0.6$ . This constraint is limited by the observational errors, and the fact that the galaxies likely have composite stellar populations, though it is consistent with presence of A stars in their spectrum. The logical extension of the correlation of FP residuals with velocity dispersion is that the cluster spirals with larger velocity dispersions, which have FP residuals of  $\Delta \log M/L_V \sim -0.3$ , must have undergone their last epochs of star-formation at  $z \sim 0.7$  (and may themselves been in an E+A phase at  $z \sim 0.5$ ).

At the present epoch, 3-4 Gyr later, the E+As should be  $\sim 0.08$  mag bluer than the  $(B-V)$  CM relation, and have faded  $\sim 1.5$  mag. Two of these galaxies are slightly brighter than  $L^*$  (using  $M_V^* \approx -21.5$  mag at  $z = 0$ ), with masses slightly lower than  $M^*$ . The third has a mass a full dex below  $M^*$ . One should therefore find the evolved counterparts of the two massive E+As in the CM relations of nearby clusters. In Figure 1 of Bower, Lucey, & Ellis (1992), one sees large scatter in  $(U-V)$  vs.  $V_T$  fainter than  $L^*$ . There is an abundance of galaxies with  $\Delta(U-V) \approx -0.16$  mag ( $\Delta(U-V) \approx 2\Delta(B-V)$ ). We conclude that the intermediate redshift star-formation in spirals, even the strong bursts thought to take place in E+A galaxies (Zabludoff *et al.* 1996), can easily be reconciled with the present-day samples of nearby early-type cluster galaxies. While these spiral galaxies may be able to hide in the normal scaling relations of early-type galaxies, the CL1358+62 E+A galaxies are less massive than  $M^*$  galaxies. We conclude that the E+A galaxies, and other low velocity dispersion early-type spirals in this CL1358+62 sample, could evolve into present-day S0 galaxies.

### 6.3. Metallicity Effects

We now explore to what extent the observed correlation in Figure 5(f) may be metallicity dependent. If the residuals are due to a systematic trend with  $\log Z$ , then, using Equations 14 and 15,

$$\Delta \log M/L_V = \frac{0.56 + 0.15 \log Z}{0.34 + 0.054 \log Z} \times \Delta(B-V) \quad (22)$$

For a sample of galaxies whose mean metallicity is solar, then  $\Delta \log M/L_V \propto 1.21 \Delta(B-V)$ . This prediction is ruled out by the least-squares fit to Figure 5(f) at the  $3-\sigma$  level.

We therefore conclude that it is the presence of young stellar populations in the spirals which in turn produce a systematic deviation of the low velocity dispersion spirals from the fundamental plane of the ellipticals. Future analysis of the metal line strengths will help determine to what extent the IMF may differ from the one adopted in the models, and to what extent metallicity variations are present in our sample.

In Equation 18 we showed the correlation expected between FP and CM residuals for old stellar populations, when variations in mean luminosity-weighted age are the primary cause of the residuals. Recall that the observed correlation for the spirals

was  $\Delta \log M/L_V \propto (2.5 \pm 0.8) \Delta(B-V)$ . Using this correlation, the single-burst models imply

$$\Delta \log Z / \Delta \log t = (-0.67_{-0.28}^{+0.16})x + (1.05_{-0.90}^{+0.50}) \quad (23)$$

An IMF with  $x = 1.35$  implies  $\Delta \log Z / \Delta \log t = 0.14_{-0.28}^{+0.52}$ , ruling out the Worthey (1994) "3/2" rule by nearly  $3-\sigma$ . If this "3/2" rule is true, then the slope of the IMF (still parameterized as a single power-law) must be  $x \sim 2.5$ . Analysis of the line-strengths is required to fully understand any correlations between luminosity-weighted age and metallicity, as well as conclusively test for variations in the initial mass function.

Though the spirals' FP is tilted with respect to the plane of the ellipticals, this can be accounted for using stellar population models. However, the residuals about the corrected plane are still quite large. This remaining scatter could be due to additional random variations in the stellar populations, such as from metallicity, or other unknown factors such as galaxy shapes, or even variable dust content.

## 7. CONCLUSIONS

The fundamental plane in the cluster CL1358+62 has been measured using accurate internal kinematics and structural parameters. In total, we have 53 cluster members, three of which have E+A spectra, and one which has emission lines, indicative of star-formation. Of the 53, 31 have been classified as E, E/S0, or S0 galaxies. There are 13 S0/a galaxies, 6 with Sa morphology, two Sab galaxies, and 1 Sb. Because our sample was selected without the use of morphology, we have made a thorough analysis of the cluster population as a whole. Several conclusions can be drawn from the current data.

(1) The 30 E, E/S0, and S0s which do not have E+A spectra or strong emission lines follow a relation which is similar in form to that found in nearby clusters:

$$\log r_e \propto (1.31 \pm 0.13) \log \sigma - (0.86 \pm 0.10) \log \langle I \rangle_e \quad (24)$$

Using these slopes, the ellipticals and S0s give identical fundamental plane zero-points, similar to the ellipticals and S0s in nearby clusters (Jørgensen, Franx, & Kjærgaard 1996). Fitting individual relations to the visually classified ellipticals and S0s does not produce significantly different results.

(2) The  $M/L_V$  ratios of the CL1358+62 early-types are lower than those in Coma by  $-0.13 \pm 0.03$  dex ( $q_0 = 0.1$ ,  $-0.10 \pm 0.03$  dex for  $q_0 = 0.5$ ). The look-back time to CL1358+62, about a third the present age of the Universe, is therefore equivalent to about  $1/4$  of the lifespan of nearby cluster galaxies, in agreement with a high mean redshift of formation for the stars in E/S0s. This comparison assumes that these Es and S0s in CL1358+62 are co-eval with those in Coma. If any contemporary E/S0 galaxies possessed later-type morphologies at intermediate redshifts, they would not have been included in the determination of this offset. Therefore, the measured  $M/L_V$  offset may only reflect a subset of contemporary E/S0 galaxies (Franx 1995).

(3) The stellar populations of early-type galaxies vary along the fundamental plane such that  $\log M/L_V \propto (2.55 \pm 0.79) \times (B-V)$ . The current data are not sufficient to specify to what extent this correlation derives from age and/or metallicity variations. If one corrects the surface brightnesses of the E/S0s for the observed correlation, the resulting plane agrees with the expectation predicted by the virial theorem and homology ( $r \propto \sigma^2 I^{-1}$ ). This result suggests that early-type galaxies form an homologous family.

(4) The E/S0 galaxies have an intrinsic  $1-\sigma$  scatter of 14% in  $V$ -band  $M/L$  ratio about the local FP slope. This scatter is consistent with the scatter in the color-magnitude relation (van Dokkum *et al.* 1998a), assuming that it is caused by a scatter in the luminosity-weighted ages of the stellar populations. The implication is that the CL1358+62 elliptical galaxies would have a scatter in mean luminosity-weighted ages of  $\sim 15\%$ , depending on the shape of the IMF. The implication is that nearly all of the star-formation in the CL1358+62 E/S0s was finished by  $z = 1$ . Measurements of Balmer and metal line strengths are required to fully understand to what extent random variations in age and metal abundance are causing scatter in the two scaling relations.

(5) The early-type spirals follow a different fundamental plane relation from the ellipticals and S0s. Given this, we studied the residuals of the spirals with respect to the fundamental plane of the ellipticals and find that the residuals of the spirals correlate with both velocity dispersion and residual from the color-magnitude relation (van Dokkum *et al.* 1998a). Thus, the spirals follow a different plane from the ellipticals and S0s because of a systematic variation of stellar populations with velocity dispersion. After several Gyr of passive stellar evolution, these spirals will follow a plane with the same form as the E/S0s, but with scatter that is twice as large.

(6) The smooth transition of color and FP residuals towards older (redder, higher  $M/L_V$  ratio) spirals indicates that star-formation has been a continuous process for these galaxies. The galaxies with the most recent star-formation have been intermediate and low velocity dispersion early-type spirals. The systematic correlation of FP residual with color, and, for example, the strong Balmer absorption lines, indicate that cluster spirals have been forming stars up through times as late as  $z \sim 0.5$ . The spiral galaxies contain composite stellar populations, and their long-term star-formation histories cannot be modeled adequately with the current data. Regardless, these galaxies clearly have a broad dispersion in properties, unlike the E/S0 galaxies.

(7) The correlation of FP residual and color residual for early-type spirals extends to the E+A galaxies, forming a tail in a sequence of recent, or recently extinguished, star-formation. That the E+A and emission line galaxies are very young and have low velocity dispersions simply places them at the extreme end of a relation between stellar populations and velocity dispersion which is specific to the spiral galaxies. Simple stellar population models imply that the mean luminosity-weighted ages of these spiral galaxies follows  $\Delta \log t \sim (1.22 - 0.28x)^{-1} \log \sigma$ . Thus, an Sa galaxy with  $\sigma = 100 \text{ km s}^{-1}$  would be about 1/4 the mean luminosity-weighted age of an Sa with  $\sigma = 300 \text{ km s}^{-1}$ , for a Salpeter (1955) IMF. However, this interpretation depends upon whatever systematic variations of luminosity-weighted ages may exist along the fundamental plane of early-type galaxies.

(8) Early-type spirals brighter than  $L^*$  at the present epoch must have formed before  $z > 1$ . Furthermore, the implication of Figure 5(e,f) is that early-type spirals with  $\sigma \gg 100 \text{ km s}^{-1}$  should show evidence for more recent star-formation at higher redshifts. This has been tentatively seen in MS1054-03 at  $z = 0.83$  (see van Dokkum *et al.* 1998b).

(9) The E+A galaxies could be as much as three times too

bright for their  $r_e$  and  $\sigma$ , compared to an extrapolation of the fundamental plane of the ellipticals. The E+As are consistent with having a burst of star-formation at  $z \sim 0.5 \pm 0.10$ . These data do not place any stronger constraints due to observational errors, and the unknown extent to which the stellar populations are composites of both old and young stars. The three E+A galaxies in the sample span a range of masses, the highest nearly the mass of an  $L^*$  galaxy, down to a full dex below  $M^*$ . By  $z \approx 0$ , these galaxies will have faded about 1.5 mag and only be  $\Delta(B-V) \approx 0.08$  mag bluer than local color-magnitude relations (*i.e.*, Bower, Lucey, & Ellis 1992), assuming these galaxies can be adequately modeled by a single, instantaneous burst. The E+As have variable bulge fractions, but invariably have disks and are partly supported by rotation (Kelson *et al.* 1999a,b, Wirth, Koo, & Kron 1994, Franx 1993). It is unlikely that they will become present-day ellipticals, but, like the other young spirals in the sample, they may evolve into S0s.

The fundamental plane has become a useful tool for studying the histories of galaxies later than E and S0 (cf. Burstein *et al.* 1997). The larger spiral fractions in clusters at higher redshift will allow for a better understanding of the evolution and transition of the spiral and early-type populations (*e.g.*, van Dokkum *et al.* 1998b). If there are processes which turn spiral galaxies into S0s between  $z = 0.33$  and  $z = 0$ , then such processes must somehow work to reduce their scatter about the fundamental plane, unless such galaxies were excluded from nearby samples for reasons other than morphology.

Future work will be aimed at measuring absorption line strengths and near-IR colors. Together with the  $V$ -band  $M/L$  ratios, one will be able to expand the modeling with the goal of disentangling composite stellar populations (*e.g.*, in the E+A galaxies), metallicities, dust contamination, the IMF, and galaxy shapes. Analysis of the fundamental plane of field galaxies at intermediate redshifts will be a very important step for comparing the evolutionary histories of early-type galaxies in different environments. Analysis of the early-types in poor groups and the field will also be important in relating the star-formation histories in intermediate environments to those in clusters and the field.

Barring the transformation of spirals into early-types, present-day cluster Es and S0s are among the oldest objects in the universe, and have undergone little, if any, late-time star formation.

We gratefully acknowledge D. Koo and S. Faber, who provided valuable comments on an early version of the paper. We also would like to acknowledge referee, G. Oemler, who helped to strengthen the presentation of this work. Furthermore, we appreciate the effort of all those in the HST program that made this unique Observatory work as well as it does. The assistance of those at STScI who helped with the acquisition of the HST data is also gratefully acknowledged. We also appreciate the effort of those at the W.M.Keck observatory who developed and supported the facility and the instruments that made this program possible. Support from STScI grants GO05989.01-94A, GO05991.01-94A, and AR05798.01-94A, and NSF grant AST-9529098 is gratefully acknowledged.

## REFERENCES

Beers, T. C., Flynn, K., & Gebhardt, K. 1990, AJ, 100, 32

Bender, R., Burstein, D., & Faber, S.M. 1992, ApJ, 399, 462

Bender, R., Burstein, D., & Faber, S.M. 1993, ApJ, 411, 153

Binney, J. & Tremaine, S. 1987, *Galactic Dynamics*, (Princeton: Princeton University Press)

Bower, R.G., Lucey, J.R., & Ellis, R.S. 1992, MNRAS, 254, 601

Burstein, D., Bender, R., Faber, S., & Nolthenius, R. 1997, AJ, 114, 1365

Caldwell, N., & Rose, J. 1997, AJ, 113, 492

Carter, D. 1987, ApJ, 312, 514

Ciotti, L., Lanzoni, B., & Renzini, A. 1996, MNRAS, 282, 1

Colless, M., Burstein, D., Davies, R.L., McMahan, R.K., Jr., Saglia, R.P., & Wegner, G. 1999, MNRAS, 303, 813

Djorgovski S., & Davis M. 1987, ApJ, 313, 59

Dressler, A. 1980, ApJ, 236, 351

Dressler A., & Gunn J. E. 1983, ApJ, 270, 7

Dressler, A., Lynden-Bell, D., Burstein, D., Davies, R.L., Faber, S.M., Terlevich, R.J., & Wegner, G 1987, ApJ, 313, 42

Dressler, A., Oemler, A., Jr., Couch, W. J., Smail, I., Ellis, R. S., Barger, A., Butcher, H., Poggianti, B. M., & Sharples, R. M. 1997, ApJ, 490, 577

Ellis R. S., Smail, I., Dressler, A., Couch, W.J., Oemler, A., Jr., Butcher, H., & Sharples, R.M. 1997, ApJ, 483, 582

Faber, S.M. & Jackson, R.E. 1976, ApJ, 204, 668

Faber S. M., Dressler A., Davies R. L., Burstein D., Lynden-Bell D., Terlevich R., & Wegner G. 1987, Faber S. M., ed., *Nearly Normal Galaxies*. Springer, New York, p. 175

Fabricant, D.G., McClintock, J.E. & Bautz, M.W. 1991, ApJ, 381, 33

Fabricant, D.G., *et al.* 1999, in preparation

Fisher, D. 1997, AJ, 113, 950

Fisher, D., Fabricant, D.G., Franx, M., & van Dokkum P.G. 1998, ApJ, 498, 195

Franx M. 1993, PASP, 105, 1058

Franx, M. 1995, IAU Symposium 164, "Stellar Populations" ed. P.C. van der Kruit & G. Gilmore (Dordrecht:Kluwer), 269

Gioia, I. M., Maccacaro, T., Schild, R. E., Wolter, A., Stocke, J. T., Morris, S. L., Henry, J. P. 1990, ApJS, 72, 567

González, J.J. 1993, Ph.D. thesis, Univ. Calif., Santa Cruz

Goudfrooij, P., de Jong, T., Hansen, L., & Nørgaard-Nielsen, H.U. 1994, MNRAS, 271, 833

Goudfrooij, P. & de Jong, T. 1995, A&A, 298, 784

Graham, A., & Colless, M. 1997, MNRAS, 287, 221

Gregg, M.D. 1989, ApJ, 337, 45

Gregg, M.D. 1992, ApJ, 384, 43

Jørgensen I., Franx M., & Kjærgaard P. 1993, ApJ, 411, 34

Jørgensen I., Franx M., & Kjærgaard P. 1996, MNRAS, 280, 167

Kauffmann, G. 1995, MNRAS, 274, 161

Kauffmann, G. 1996, MNRAS, 281, 487

Kelson, D.D. 1998, Ph.D. thesis, Univ. of California, Santa Cruz

Kelson, D.D. van Dokkum, P.G., Franx, M., Illingworth, G.D., & Fabricant, D.G. 1997, ApJL, 478, L13

Kelson, D.D., Illingworth, G.D., van Dokkum, P.G., & Franx, M. 1999a, ApJ, *submitted*

Kelson, D.D., Illingworth, G.D., van Dokkum, P.G., & Franx, M. 1999b, ApJ, *submitted*

Kelson, D.D. *et al.* 1999c, ApJ, *submitted*

Kelson, D.D. 1999, ApJ, *in preparation*

Koo, D.C. & Kron, R. 1992, ARA&A, 30, 613

Kuntschner, H. & Davies R.L. 1998, MNRAS, 295, 29

Leitherer, C. *et al.* 1996, PASP, 108, 996

Lilly S. J., Tresse L., Hammer F., Crampton D., & Le Fèvre O. 1995, ApJ, 455, 50

Lucey, J.R., Bower, R.G., & Ellis, R.S. 1991, MNRAS, 249, 755

Oemler, A., Jr. 1974, ApJ, 194, 10

Oke, J.B., *et al.* 1995, PASP, 107, 375

Pahre, M.A. 1998, Ph.D. thesis, California Inst. of Technology

Pahre, M. A. & Djorgovski, S. G. 1996, in *Proceedings of the Second Stromlo Symposium, The Nature of Elliptical Galaxies*, M. Arnaboldi, G. S. Da Costa, & P. Saha, eds., in press

Pahre, M. A., Djorgovski, S. G., & de Carvalho, R. R. 1995, ApJL, 453, L17

Pahre, M. A., Djorgovski, S. G., & de Carvalho, R. R. 1998, AJ, *submitted*

Prugniel, Ph. & Simien, F. 1996, A&A, 309, 749

Rix, H.-W. & White, S.D.M. 1990, ApJ, 362, 52

Saglia, R.P., Bender, R., & Dressler, A. 1993, A&A, 279, 75

Saglia, R.P., *et al.* 1997, ApJS, 109, 79

Salpeter, E.E. 1955, ApJ, 121, 161

Sandage, A.R., & Visvanathan, N. 1978, ApJ, 225, 742

Schade, D., Carlberg, R.G., Yee, H.K.C. & López-Cruz, O. 1997, ApJL, 477, L17

Sersic, J.L. 1968, *Atlas de Galaxias Australes*, (Cordoba: Observatorio Astronomico)

Stanford, S.A., Eisenhardt, P.R., & Dickinson, M. 1998, ApJ, 492, 461

Terlevich, R.J., Davies, R.L., Faber, S.M. & Burstein, D. 1981, MNRAS, 196, 381

Tinsley, B.M. & Gunn, J.E. 1976, ApJ, 203, 52

Trager, S.C., *et al.* 1999, in preparation

Tsai, J.C. & Mathews, W.G. 1996, ApJ, 468, 571

Tully, R.B. & Fisher J.R. 1977, A&A, 54, 661

van Dokkum, P. G., & Franx M. 1995, AJ, 110, 2027

van Dokkum, P. G., & Franx M. 1996, MNRAS, 281, 985

van Dokkum, P.G., Franx, M., Illingworth, G. D., Kelson, D. D., Fisher, D., & Fabricant, D. 1998a, ApJ, 500, 714

van Dokkum, P. G., Franx, M., Kelson, D. D., & Illingworth, G. D. 1998b, ApJ, 504, L17

Vogt, N. P., Forbes, D. A., Phillips, A. C., Gronwall, C., Faber, S. M., Illingworth, G. D., & Koo, D. C. 1996, ApJL, 465, L15

Vogt, N. P., Phillips, A. C., Faber, S. M., Gallego, J., Gronwall, C., Guzmán, R., Illingworth, G. D., Koo, D. C., & Lowenthal, J.D. 1997, ApJL, 479, L121

Wegner, G., Colless, M., Bagley, G., Davies, R.L., Bertschinger, E., Burstein, D., McMahan, R.K., Jr., & Saglia, R.P. 1996, ApJS, 106, 1

Wirth, G.D., Koo, D.C., & Kron, R.G. 1994, ApJL, 435, L105

Worley, G. 1994, ApJS, 95, 107

Worley, G., Trager, S. C., & Faber, S. M. 1996, in "Fresh Views on Elliptical Galaxies," eds. A. Buzzoni, A. Renzini, & A. Serrano, (ASP Conf. Ser., 86) p. 203

Zabludoff, A.I. *et al.* 1996, ApJ, 466, 104

Ziegler, B. L., & Bender, R. 1997, MNRAS, 291, 527

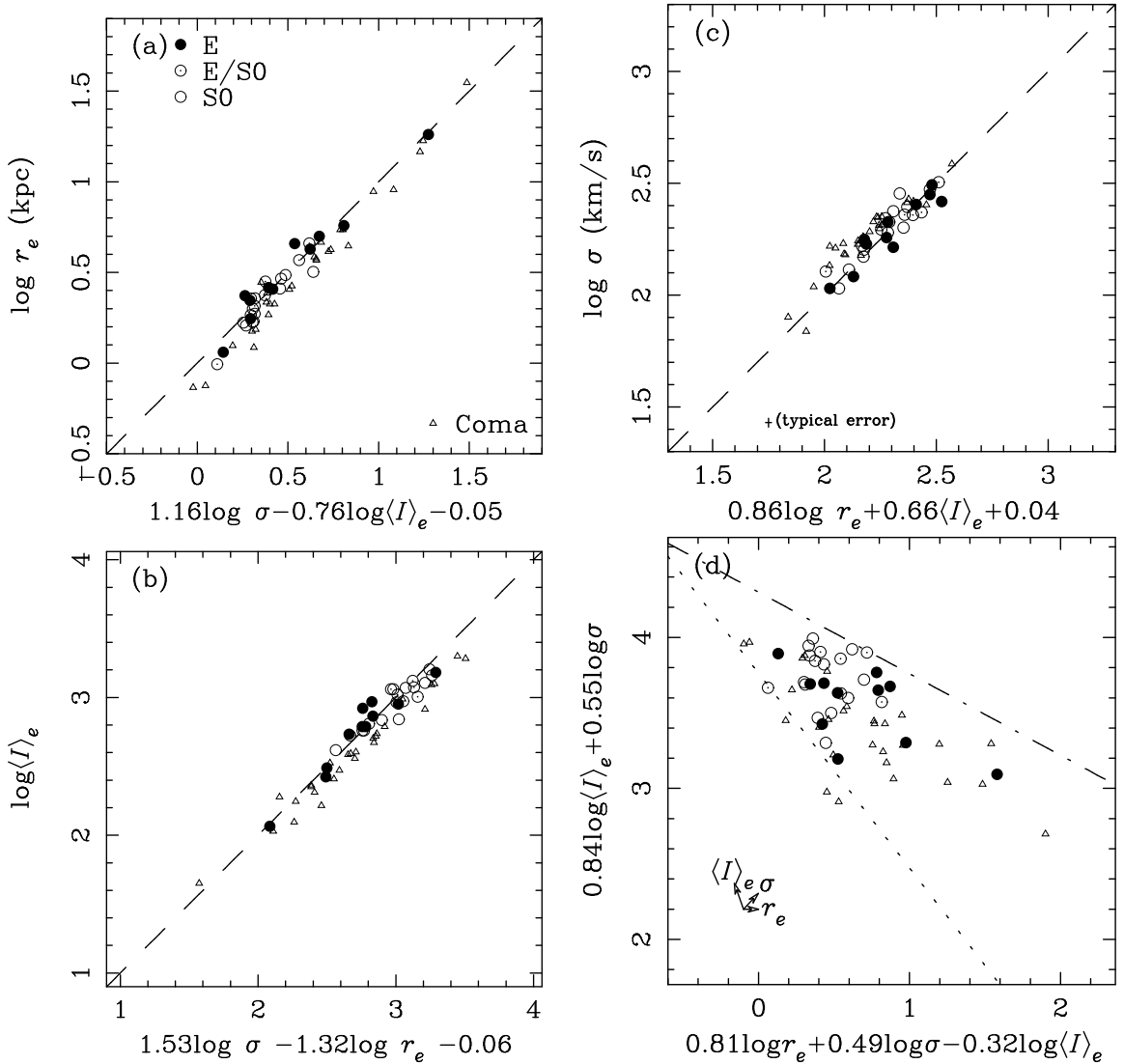


FIG. 1.— The fundamental plane of early-type galaxies in CL1358+62. In (a-c) we show the long, intermediate, and short edge-on views and in (d) the face-on distribution. The early-type galaxies clearly form a tight relation in (a-c). The dashed lines show the fit to the elliptical galaxies of CL1358+62. In (c), we show the size of a typical error. The absence of galaxies in the lower left region of (d) is attributed to the magnitude limit of the sample, denoted by the dotted line. The absence of galaxies in the upper right is referred to as the “Zone of Avoidance” (Bender, Burstein, & Faber 1993). The CL1358+62 galaxies are shown by the large symbols indicated in (a). The Coma V-band sample is shown by small triangles (Jørgensen, Franx, & Kjærgaard 1996).

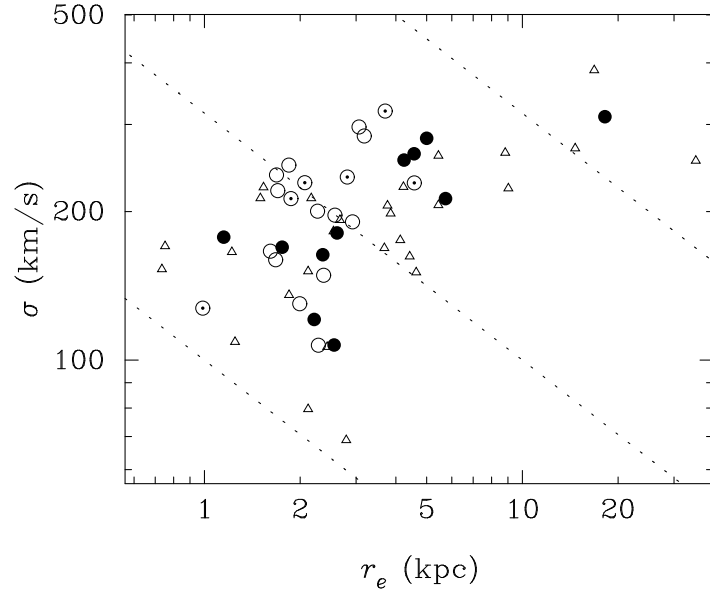


FIG. 2.— The log  $\sigma$ -log  $r_e$  plane in CL1358+62 vs. the Coma sample (Jørgensen, Franx, & Kjærgaard 1996). The symbols are as in Figures 1. Contours of constant mass ( $5\sigma^2 r_e / G = 10^{10,11,12} M_\odot$ , Bender, Burstein, & Faber 1992) are shown by the dotted lines. The distribution of early-type galaxy masses at  $z = 0.33$  appears remarkably similar to the  $V$ -band early-type sample in Coma.

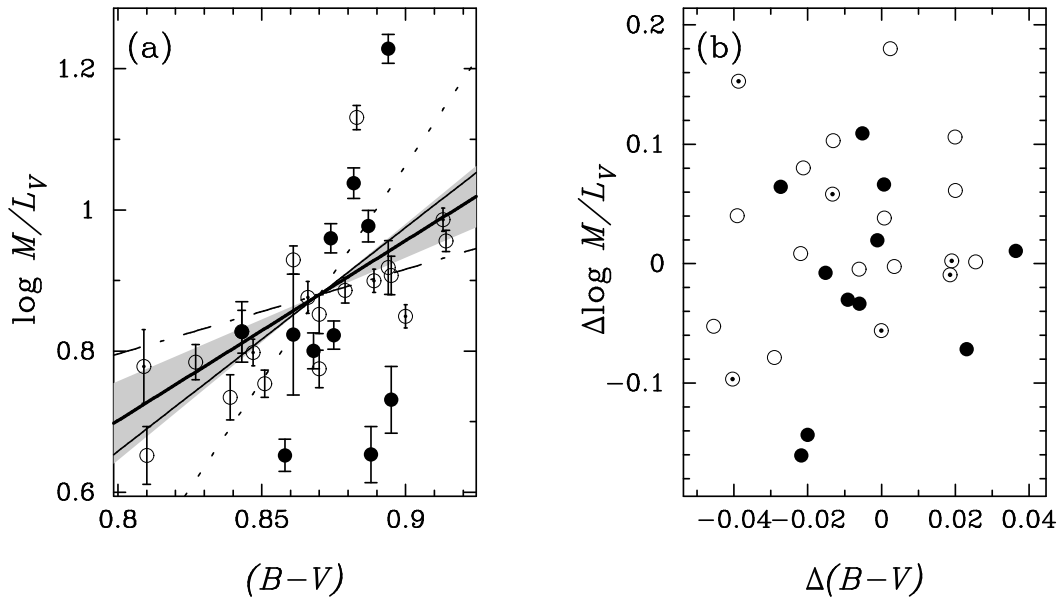


FIG. 3.— (a)  $M/L_V$  ratios are shown plotted against  $(B-V)$  colors for the early-type galaxies. A Spearman rank test indicates a 99.9% probability that  $M/L_V$  ratios are correlated with galaxy color. The linear-least squares fit gives a slope of  $2.55 \pm 0.79$ , as shown by the thick solid line. The  $1-\sigma$  uncertainties are shown by the enclosed gray region. The thin solid line is the slope expected for systematic age variations, the thin dash-dot line for pure metallicity variations. The slope predicted by the Worthey (1994) "3/2" rule is shown by the thin dotted line. Typical color uncertainties are  $\pm 0.011$  mag (van Dokkum *et al.* 1998a). In (b) fundamental plane residuals are plotted against the residuals from the  $(B-V)$  color-magnitude relation and no significant correlation is seen.

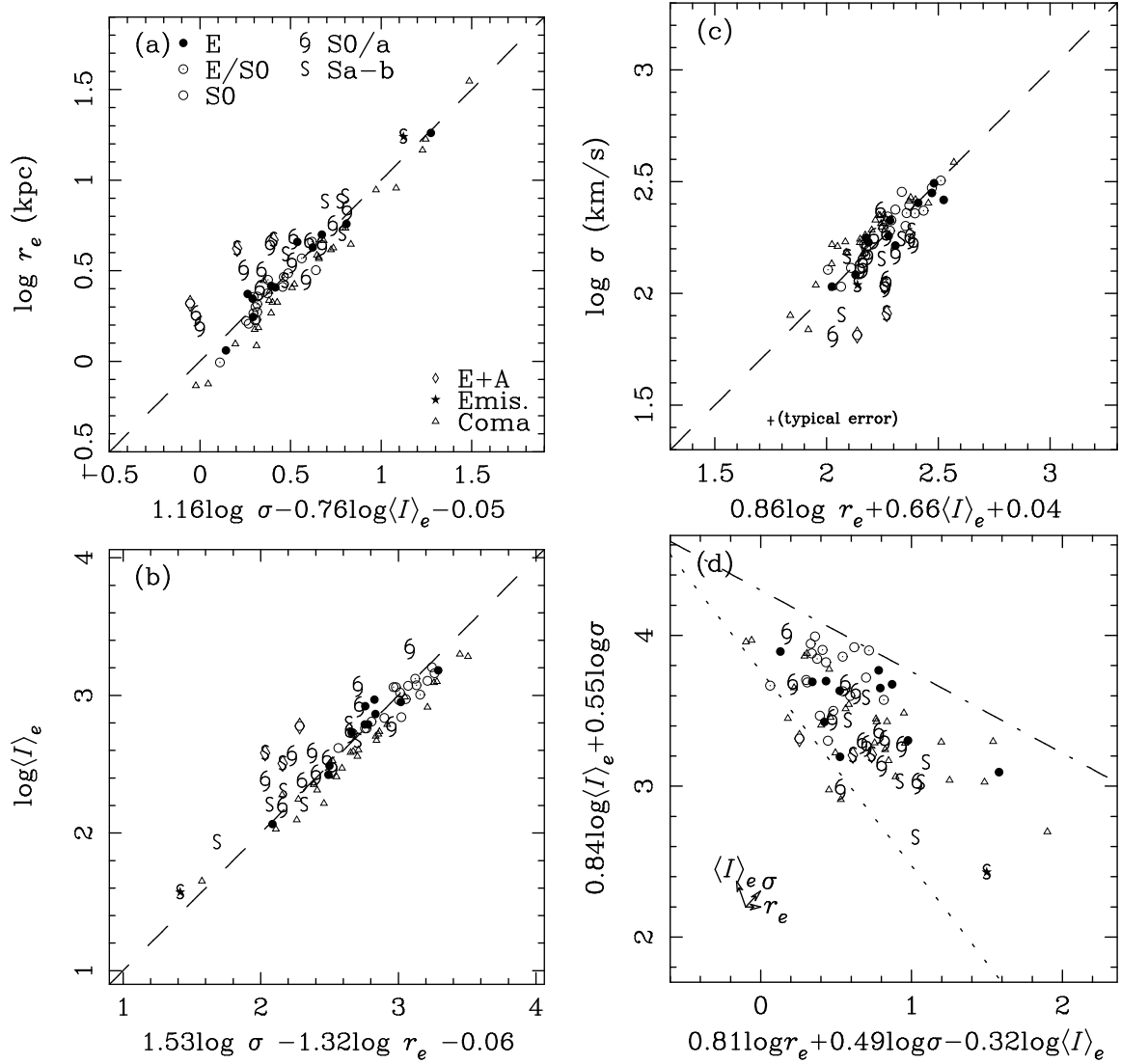


FIG. 4.— (a-d) The full sample of 53 galaxies are shown together. Note that the later-type galaxies are systematically brighter than the plane of the early-types.

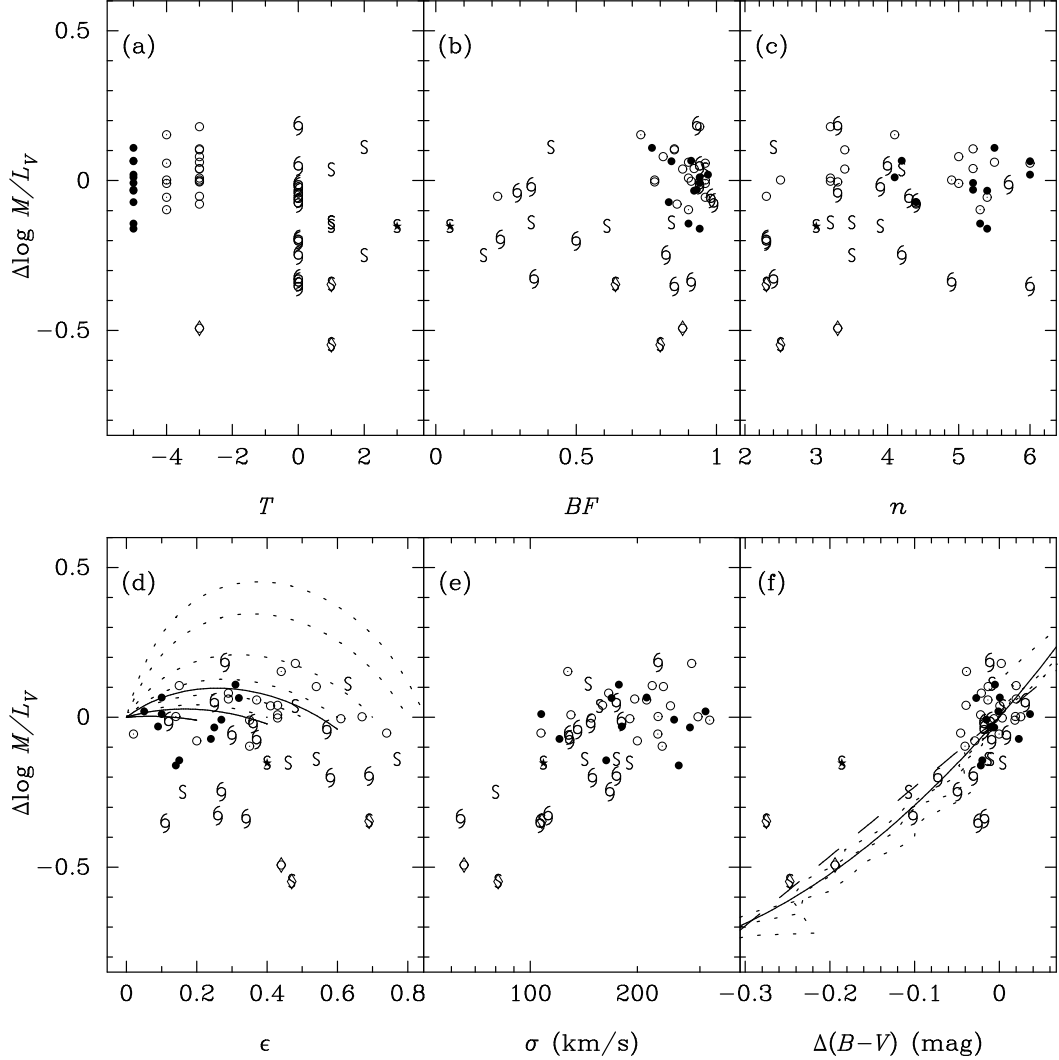


FIG. 5.— Fundamental plane residual as a function of (a)  $T$ , galaxy morphology, as determined in Fabricant *et al.* (1998); (b) bulge fraction, derived from bulge-plus-disk decompositions of the integrated surface brightness profiles; (c)  $n$ , the shape parameter describing the best-fit  $r^{1/n}$ -law; (d) apparent ellipticity superimposed with curves following the random projection of simple models described in the text; (e) central velocity dispersion; and (f) residual from the color-magnitude relation (van Dokkum *et al.* 1998a), superimposed with models of single-burst stellar populations with three different metallicities ( $[\mathrm{Z}/\mathrm{H}] = -0.4, 0.0, +0.4$ ). The models, normalized to a redshift of formation of  $z = 2$  ( $H_0 = 65 \text{ km s}^{-1} \text{Mpc}^{-1}$ ,  $q_0 = 0.1$ ) at zero residual, are shown as dotted lines. The least-squares fit to the spirals without emission or strong Balmer absorption of  $\Delta \log M/L_V \propto 2.5\Delta(B-V)$  is shown as the dashed line. The analytical approximation to a solar metallicity,  $x = 1.35$ , single-burst stellar population is shown as the solid line. There is a clear trend of  $M/L_V$  residual with galaxy morphology, central velocity dispersion, and color. The symbols are as in Figures 1 and 4.

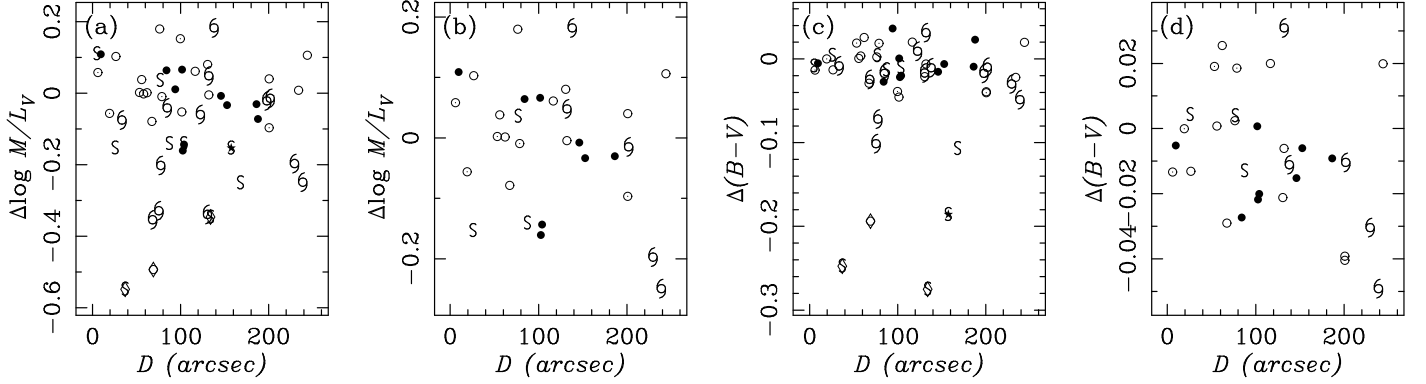


FIG. 6.— Fundamental plane residuals plotted vs. distance from the cD for (a) the full sample, and (b) for those galaxies with  $\sigma \geq 150 \text{ km s}^{-1}$ . In (c) and (d), the color-magnitude relation residuals are shown in the same manner. At the distance of the cluster, the scale is  $4.8 \text{ kpc/arcsec}$ . No significant correlation of fundamental plane residual with distance from the cD is seen.

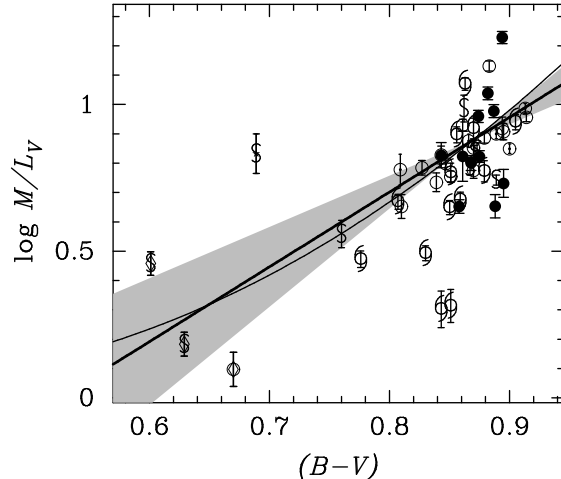


FIG. 7.—  $M/L_V$  ratios are shown plotted against  $(B-V)$  colors for the full sample. The linear-least squares fit from §4 is shown by the thick solid line and enclosed gray region. For a Salpeter (1955) IMF, and solar metallicities, one expects the  $M/L_V$  ratio and  $(B-V)$  colors to evolve along paths parallel to the thin solid line.

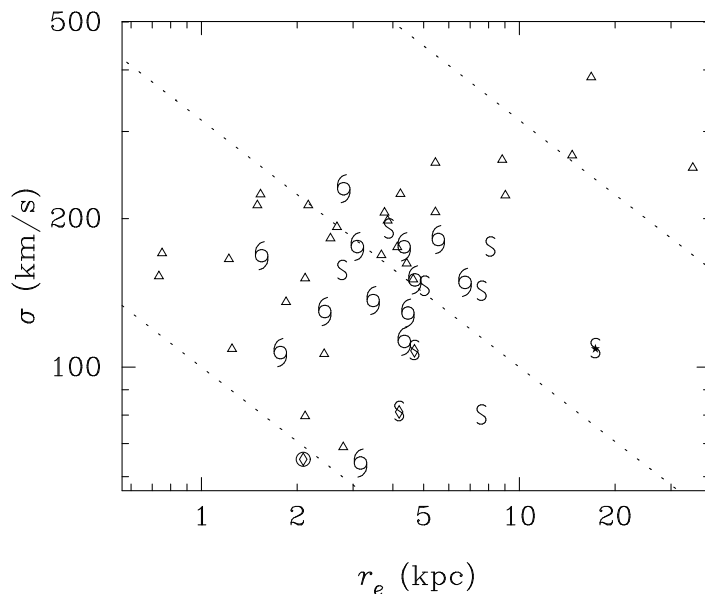


FIG. 8.— Similar to the E/S0s shown in Figure 2, the later-type galaxies in our sample also have mass and length scales which are comparable to those seen in the local sample. As in Fig. 2, contours of constant mass ( $5\sigma^2 r_e / G = 10^{10,11,12} M_\odot$ ) are shown by the dotted lines.

TABLE 1  
DATA USED IN THE CL1358+62 FUNDAMENTAL PLANE

ID	Type	$n$	$\sigma$	$r_e$	$\langle \mu_e \rangle$	$R$	$(B-V)_z$	ID	Type	$n$	$\sigma$	$r_e$	$\langle \mu_e \rangle$	$R$	$(B-V)_z$
095	S0	5.2	220.5	0.356	19.84	20.18	0.894	359	S0	4.4	200.3	0.475	19.95	20.14	0.851
...	...	$\pm 1.2$	$\pm 6.4$	$\pm 0.004$	$\pm 0.02$	...	...	...	...	$\pm 0.4$	$\pm 4.5$	$\pm 0.005$	$\pm 0.02$	...	...
110	S0/a	2.3	174.8	0.648	20.32	19.87	0.850	360	E	5.5	177.5	0.241	19.65	20.74	0.861
...	...	$\pm 0.3$	$\pm 3.7$	$\pm 0.012$	$\pm 0.04$	...	...	...	...	$\pm 0.5$	$\pm 19.7$	$\pm 0.004$	$\pm 0.03$	...	...
129	S0/a	4.2	167.5	0.324	19.27	19.94	0.830	366	S0/a	3.3	228.9	0.587	20.63	20.31	0.863
...	...	$\pm 0.2$	$\pm 3.8$	$\pm 0.004$	$\pm 0.02$	...	...	...	...	$\pm 0.3$	$\pm 6.4$	$\pm 0.005$	$\pm 0.03$	...	...
135	S0	5.2	159.7	0.351	20.19	20.59	0.827	368	Sab	2.4	145.6	1.055	22.09	20.33	0.862
...	...	$\pm 0.2$	$\pm 5.1$	$\pm 0.009$	$\pm 0.05$	...	...	...	...	$\pm 2.6$	$\pm 7.5$	$\pm 0.032$	$\pm 0.06$	...	...
142	S0/a	3.9	147.9	1.414	22.15	20.16	0.856	369	S0/a	4.3	128.2	0.935	21.70	20.51	0.879
...	...	$\pm 0.9$	$\pm 4.4$	$\pm 0.046$	$\pm 0.07$	...	...	...	...	$\pm 0.3$	$\pm 6.1$	$\pm 0.023$	$\pm 0.05$	...	...
164	S0/a	5.7	180.6	1.165	21.56	19.83	0.870	371	Sa	3.5	174.8	1.699	21.84	20.02	0.871
...	...	$\pm 0.7$	$\pm 4.3$	$\pm 0.035$	$\pm 0.06$	...	...	...	...	$\pm 1.5$	$\pm 4.0$	$\pm 0.033$	$\pm 0.04$	...	...
182	S0	3.2	130.1	0.418	20.70	20.82	0.839	372	Sa	3.2	142.3	1.595	22.09	20.02	0.867
...	...	$\pm 0.2$	$\pm 5.4$	$\pm 0.008$	$\pm 0.04$	...	...	...	...	$\pm 1.2$	$\pm 5.0$	$\pm 0.064$	$\pm 0.08$	...	...
209	Sa	2.3	107.9	0.980	21.34	19.99	0.601	375	E	6.0	311.3	3.813	22.44	19.09	0.894
...	...	$\pm 0.3$	$\pm 5.2$	$\pm 0.018$	$\pm 0.04$	...	...	...	...	$\pm 0.1$	$\pm 7.0$	$\pm 0.075$	$\pm 0.04$	...	...
211	S0	3.3	190.5	0.612	20.58	20.14	0.870	381	E/S0	6.0	212.4	0.392	19.92	19.99	0.866
...	...	$\pm 0.3$	$\pm 6.4$	$\pm 0.015$	$\pm 0.05$	...	...	...	...	$\pm 0.1$	$\pm 5.5$	$\pm 0.009$	$\pm 0.04$	...	...
212	E	5.2	181.0	0.547	20.44	20.08	0.868	397	S0/a	3.3	135.9	0.727	21.29	20.52	0.851
...	...	$\pm 0.2$	$\pm 5.7$	$\pm 0.009$	$\pm 0.03$	...	...	...	...	$\pm 0.3$	$\pm 5.1$	$\pm 0.020$	$\pm 0.06$	...	...
215	S0	5.0	166.2	0.338	20.17	20.74	0.843	408	S0	3.4	237.1	0.353	19.70	20.20	0.861
...	...	$\pm 1.0$	$\pm 5.9$	$\pm 0.006$	$\pm 0.03$	...	...	...	...	$\pm 0.4$	$\pm 6.2$	$\pm 0.003$	$\pm 0.02$	...	...
233	E/S0	5.3	234.9	0.590	19.95	19.36	0.847	409	E	4.1	107.3	0.536	21.38	21.17	0.895
...	...	$\pm 0.3$	$\pm 4.5$	$\pm 0.012$	$\pm 0.04$	...	...	...	...	$\pm 1.1$	$\pm 6.7$	$\pm 0.005$	$\pm 0.02$	...	...
234	Sb	3.0	108.9	3.656	23.68	20.08	0.689	410	S0	3.2	148.6	0.497	20.70	20.78	0.870
...	...	$\pm 1.0$	$\pm 8.2$	$\pm 0.349$	$\pm 0.18$	...	...	...	...	$\pm 0.2$	$\pm 5.2$	$\pm 0.008$	$\pm 0.03$	...	...
236	S0	5.5	196.7	0.539	20.51	20.20	0.895	412	E	6.0	169.4	0.369	20.22	20.48	0.843
...	...	$\pm 1.5$	$\pm 5.6$	$\pm 0.009$	$\pm 0.03$	...	...	...	...	$\pm 0.1$	$\pm 6.3$	$\pm 0.007$	$\pm 0.04$	...	...
242	E	4.2	212.4	1.201	21.54	19.96	0.882	433	S0/a	6.0	106.6	0.371	19.95	20.21	0.851
...	...	$\pm 0.2$	$\pm 5.3$	$\pm 0.026$	$\pm 0.04$	...	...	...	...	$\pm 0.1$	$\pm 4.0$	$\pm 0.011$	$\pm 0.06$	...	...
256	E	5.4	261.8	0.956	20.30	18.96	0.875	440	S0/a	4.9	63.7	0.663	21.67	20.96	0.843
...	...	$\pm 0.4$	$\pm 4.3$	$\pm 0.010$	$\pm 0.02$	...	...	...	...	$\pm 0.9$	$\pm 5.0$	$\pm 0.016$	$\pm 0.05$	...	...
269	E/S0	5.0	319.5	0.776	20.05	19.12	0.913	454	S0/a	2.3	149.6	0.983	21.16	19.96	0.807
...	...	$\pm 1.0$	$\pm 5.8$	$\pm 0.008$	$\pm 0.02$	...	...	...	...	$\pm 0.3$	$\pm 3.7$	$\pm 0.014$	$\pm 0.03$	...	...
292	S0/a	2.4	112.3	0.911	21.21	20.14	0.776	463	S0	3.2	284.4	0.667	20.50	19.99	0.883
...	...	$\pm 0.4$	$\pm 3.2$	$\pm 0.031$	$\pm 0.07$	...	...	...	...	$\pm 0.2$	$\pm 6.4$	$\pm 0.007$	$\pm 0.02$	...	...
298	S0	2.5	296.6	0.642	19.93	19.47	0.914	465	Sa	4.2	156.7	0.581	20.93	20.61	0.873
...	...	$\pm 0.5$	$\pm 5.2$	$\pm 0.007$	$\pm 0.02$	...	...	...	...	$\pm 0.2$	$\pm 5.0$	$\pm 0.009$	$\pm 0.03$	...	...
300	S0	3.4	248.2	0.386	19.59	19.98	0.879	481	S0	2.3	107.2	0.478	21.06	21.07	0.810
...	...	$\pm 0.4$	$\pm 5.5$	$\pm 0.004$	$\pm 0.02$	...	...	...	...	$\pm 0.3$	$\pm 5.5$	$\pm 0.015$	$\pm 0.06$	...	...
303	E	5.3	163.5	0.494	20.18	19.95	0.858	493	E/S0	4.1	127.5	0.207	20.09	21.59	0.809
...	...	$\pm 0.3$	$\pm 4.3$	$\pm 0.007$	$\pm 0.03$	...	...	...	...	$\pm 1.1$	$\pm 8.8$	$\pm 0.010$	$\pm 0.10$	...	...
309	E/S0	4.9	228.7	0.433	19.80	19.84	0.900	523	S0/a	4.0	174.6	0.910	21.42	20.36	0.905
...	...	$\pm 0.9$	$\pm 4.7$	$\pm 0.003$	$\pm 0.01$	...	...	...	...	$\pm 1.0$	$\pm 5.9$	$\pm 0.016$	$\pm 0.04$	...	...
328	Sa	2.5	81.2	0.878	21.15	19.96	0.629	531	E	5.4	281.3	1.048	20.63	19.33	0.887
...	...	$\pm 0.5$	$\pm 4.2$	$\pm 0.016$	$\pm 0.04$	...	...	...	...	$\pm 0.4$	$\pm 5.0$	$\pm 0.009$	$\pm 0.02$	...	...
335	S0/a	4.4	129.1	0.512	20.79	20.47	0.859	534	E	4.4	120.9	0.464	20.77	20.73	0.888
...	...	$\pm 0.4$	$\pm 4.3$	$\pm 0.009$	$\pm 0.04$	...	...	...	...	$\pm 0.4$	$\pm 6.1$	$\pm 0.008$	$\pm 0.04$	...	...
343	S0	3.3	65.1	0.438	20.66	20.66	0.670	536	E	5.2	254.1	0.890	20.63	19.70	0.874
...	...	$\pm 0.3$	$\pm 5.0$	$\pm 0.010$	$\pm 0.05$	...	...	...	...	$\pm 0.2$	$\pm 5.0$	$\pm 0.009$	$\pm 0.02$	...	...
353	E/S0	5.4	228.5	0.958	20.79	19.50	0.889	549	Sab	3.5	79.9	1.592	22.77	20.66	0.760
...	...	$\pm 0.4$	$\pm 4.4$	$\pm 0.007$	$\pm 0.01$	...	...	...	...	$\pm 0.5$	$\pm 4.6$	$\pm 0.058$	$\pm 0.07$	...	...
356	Sa	3.9	190.2	0.815	20.62	19.66	0.889	...	...	...	...	...	...	...	...
...	...	$\pm 0.1$	$\pm 3.7$	$\pm 0.011$	$\pm 0.03$	...	...	...	...	...	...	...	...	...	...

NOTE.— Velocity dispersions from Kelson *et al.* (1999a). The effective radii are given in arcsec. Surface brightnesses are in  $V_z$  magnitudes per square arcsec, where  $V_z$  is equivalent to the Johnson  $V$  filter redshifted to the observed frame of the galaxies (Kelson *et al.* 1999b). The formal uncertainties in these structural parameters are reported above, and, although the systematic errors in either parameter can be quite large, their combined error in the fundamental plane is quite small. Morphologies are from Fabricant *et al.* (1999), and  $(B-V)_z$  colors are from van Dokkum *et al.* (1998a). The colors are likely to be uncertain at a level of  $\pm 0.02$  mag. The  $R$  magnitudes are from Fabricant, McClintock, & Bautz (1991).